Gold(I) Complexes of Ferrocenyl Polyphosphines: Aurophilic Gold Chlorides Formation and Phosphine-Concerted Shuttling of a Dinuclear [ClAu•••AuCl] Fragment

Vincent Rampazzi, Julien Roger, Régine Amardeil, Marie-José Penouilh, Philippe Richard, Paul Fleurat-Lessard, Jean-Cyrille Hierso

Gold(I) Complexes of Ferrocenyl Polyphosphines: Aurophilic Gold Chlorides Formation and Phosphine-Concerted Shuttling of a Dinuclear [ClAu•••AuCl] Fragment

Vincent Rampazzi,[a] Julien Roger,[a] Régine Amardeil,[a] Marie-José Penouilh,[a] Philippe Richard,[a] Paul Fleurat-Lessard, [a] and Jean-Cyrille Hierso[a,b]*

[a]Université de Bourgogne Franche-Comté, Institut de Chimie Moléculaire de l'Université de Bourgogne (ICMUB UMR 6302 CNRS) – 9 Avenue Alain Savary, 21078 Dijon, France

[b]Institut Universitaire de France (IUF), 103 Boulevard Saint Michel, 75005 Paris Cedex, France

ABSTRACT

A smart steric control of the metallocene backbone in di- and poly(phosphino) ferrocene ligands favors intramolecular aurophilic interactions between [AuCl] fragments in polynuclear gold(I) complexes. We synthesized and characterized by multinuclear NMR and XRD analysis mono-, di- and polynuclear gold complexes of constrained ferrocenyl diphosphines, which bear either bulky *tert*-butyl groups or more flexible siloxane substituents at the cyclopentadienyl rings. The complexes *meso*-1,1'-bis(diphenylphosphino)-3,3'-di-*tert*-butyl ferrocene (**4-m**), *rac*-1,1'-bis[di(5-methyl-2-furyl)phosphino]-3,3'-di-*tert*-butyl ferrocene (**5-r**), *rac*-1,1'-bis(diphenylphosphino)-3,3'-(tri-*iso*-propylsilyloxy) ferrocene (**6-r**) were used to form dinuclear gold complexes. The coordination of *tert*-butylated ferrocenylphosphines generated aurophilic interactions in the corresponding dinuclear gold complexes, contrary to gold(I) complexes reported with 1,1'-bis(diphenylphosphino)ferrocene (dppf). The structurally related tetraphosphine 1,1',2,2'-tetrakis(diphenylphosphino)-4,4'-di-*tert*-butylferrocene (**11**) also gave access to mono-, di- and original trinuclear gold chloride aurophilic complexes in which $14e^-$ to $16e^-$ gold centers co-exist. In such complexes nonbonded ("through-space") $^{31}P–^{31}P'$ nuclear spin couplings were evidenced by high resolution NMR. In these interactions nuclear spin information is transferred between the lone-pair electron of an uncoordinated phosphorous P and a phosphorous P' that is involved in a σ covalent bond Au–P'. The dinuclear aurophilic complex displayed a concerted shuttling of its [ClAu···AuCl] fragment between the four phosphorus donors of the tetraphosphine ligand. Thus, an aurophilic Au•••Au bond, which is assumed to be a weak energy interaction, can be conserved within a dynamic shuttling process at high temperature involving an intramolecular coordination–decoordination process of digold(I) at phosphorus atoms.

INTRODUCTION

Weak attractive interactions between closed shell metal ions have been studied in relation with both intra- and intermolecular species.[1] Attractive closed-shell interactions between d10–d10 pairs of gold atoms have especially received increasing attention, and new properties and reactivity have been lately evidenced.[2] Aurophilic interaction designates situations in which these heavy metal atoms come close to each other with the formation of attractive Au···Au interaction identified in the solid state by using X-ray diffraction structural data. These provide accurate information about the distance between the metals involved, typically ranging between *ca.* 2.55–3.40 Å.[3] The strength of such metal–metal interactions is comparable to that of hydrogen bonding (*ca.* 5–10 kcal.mol^{-1}) and can be enough to bring about novel bonding and structural features, and confer valuable physical properties.[4] The weak magnitude of Au···Au interaction could be unfavorably affected by a variety of competing effects. Indeed, the positive interaction between two gold atoms has been readily overcome by other structurally determining factors, such as steric hindrance, dipole interactions, charge effects, hydrogen bonding or electrostatics.[5] Long range gold…gold separations have been reported in metallic dimers and polymers of metallocenic halide gold(I) complexes (Chart 1, top). Those structures clearly preclude any possible aurophilic interactions (**1**-**2**).[6,7] On the other hand, intramolecular aurophilic bondings have been observed in a range of compounds with formula [(L(Au)$_2$(μ-dppf)] (dppf =1,1'-bis[diphenylphosphino]ferrocene, Chart 1, bottom) with L being a monodentate ligand (other than halides) such as 2-mercaptobenzamide (**3a**),[8] 2-(dimethylaminomethyl)phenylselenolato (**3b**),[9] (*Z*)-*O*-*iso*-propyl-*N*-(4-nitrophenyl)thiocarbamato,[10] *O*-methyl-*N*-(4-nitrophenyl)thiocarbamide,[11] and 2,2'-bipyridin-5-ylethynyl (**3c**).[12] Compound [(ClAu)$_2$(μ-DHNPFc)] (DHNPFc = 1,1'-bis(1,4-

dihydrodinaphtho[2,1-d:1',2'-g]-[1,3,6,2]dioxathiaphosphocinyl)ferrocene) also shows substantial intramolecular aurophilic interactions.[13] The ancillary ligand L is apparently essential for forming aurophilic bonds. The factors insuring the formation of aurophilic interactions in digold(I) complexes are far from being fully understood and mastered.

Chart 1. Representative Digold(I) Complexes Stabilized by Metallocenic Diphosphines

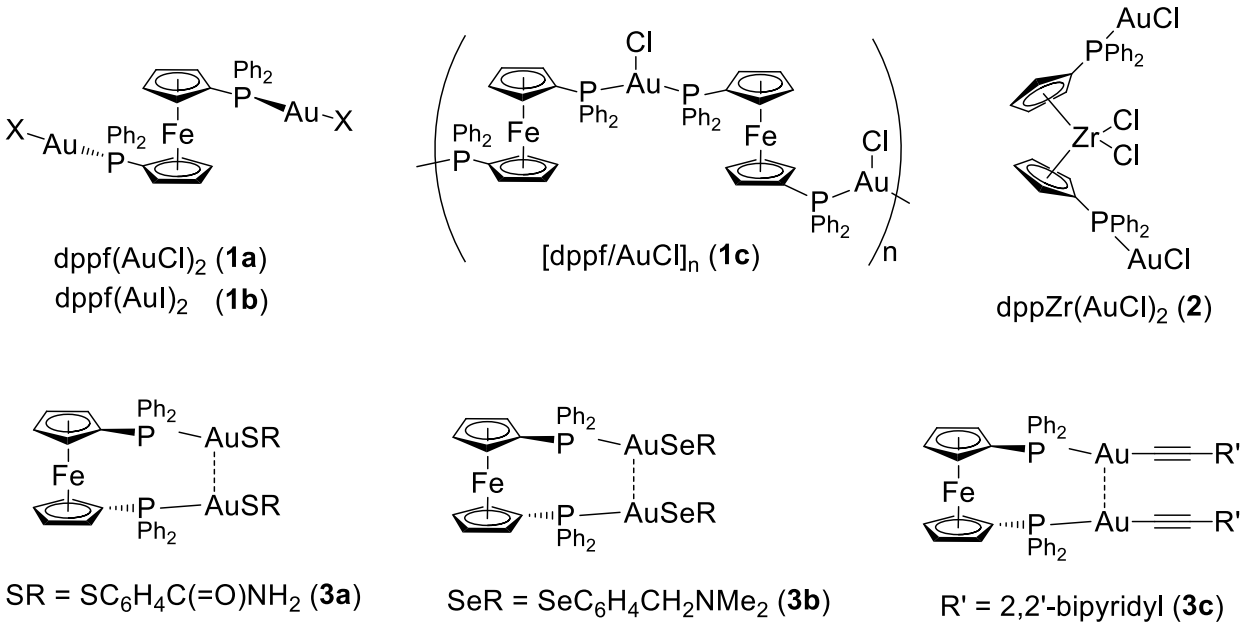

We hypothesized that a smart conformation control in poly(phosphino) ferrocene ligands may favor intramolecular aurophilic interactions between [Au^{I}Cl] fragments in polynuclear gold(I) complexes. We investigated the formation of gold(I) complexes from various constraint ferrocenyl diphosphines and extended our study to related tetraphosphine gold(I) complexes of various nuclearity. The structurally related tetraphosphine 1,1',2,2'-tetrakis(diphenylphosphino)-4,4'-di-*tert*-butylferrocene (**11**) generated gold mononuclear and polynuclear complexes. Nonbonded ("through-space") ^{31}P–^{31}P nuclear spin couplings involving non classical interactions between the electrons of a σ(Au–P) covalent bond and the lone-pair of an uncoordinated

phosphorus were evidenced for the first time. In such polynuclear complexes aurophilic interactions displayed also a concerted dynamic behavior with a shuttling of the digold moiety between four phosphorus donors. An aurophilic interaction in an appropriately constrained arrangement can be conserved within a dynamic behavior at elevated temperature, despite its only weak energy bonding.

RESULTS AND DISCUSSION

Gold(I) Complexes of Constrained Ferrocenyl Diphosphines. In the course of our studies on the physical,[14] and chemical properties[15] of ferrocenyl-based polyphosphine ligands with transition metals we previously examined within group 11 metals the formation of Cu(I) iodide adducts with ferrocenyl tri- and tetraphosphines.[16] Polynuclear copper halide complexes were not formed, but mononuclear tetraligated Cu(I) adducts allowed Sonogashira reaction to be conducted in the presence of unexpectedly low amounts of copper co-catalyst (0.4 to 0.1 mol%). In contrast to Cu(I) coordination chemistry, gold(I) polynuclear metal complexes might be synthesized using polydentate ferrocenyl phosphines. Such gold complexes are relevant in relation with their potential aurophilic properties. A better structural control towards formation of di- and polynuclear gold complexes may be achieved using ferrocenyl polyphosphines.

The pioneering studies from the groups of Hill,[7] Laguna,[17] Hor,[18] and others,[19] have shown that digold(I) chloride complexes can be formed by coordination of the diphosphine dppf to Au–X fragments (X = Cl, I); these complexes showed no *intramolecular* Au···Au interaction in the solid state. Hill observed the co-crystallization of two molecules, from which one displayed no Au···Au interaction (Chart 1, complexes **1a**) and the other displayed intermolecular Au···Au close contacts.[7] The works from Laguna group confirmed the formation of [dppf$(AuCl)_2$] (**1a**) and its

iodide analog (**1b**); they did not observed any intermolecular interaction.[17] The polymeric $[dppf/AuCl]_n$, (Chart 1, **1c**) was obtained by Hor *et al.* when dppf was added in a 1:1 ratio to $[AuCl(SMe_2)]$ in CH_2Cl_2.[18] In our case we also obtained the polymeric species (**1c**) (FIGSI1 in SI) from 1:1 and also from 1:2 molar ratio of dppf reacted with $[AuCl(SMe_2)]$.

A specific orientation of phosphine donors may be favorable to produce dinuclear metallic species with closer gold centers location. We synthesized polysubstituted ferrocenyl diphosphines (Chart 2), which were reacted with one or two equiv. of $[AuCl(SMe_2)]$ under standardized conditions.

Chart 2. Polysubstituted 3,3'- Ferrocenyl 1,1'-Diphosphines

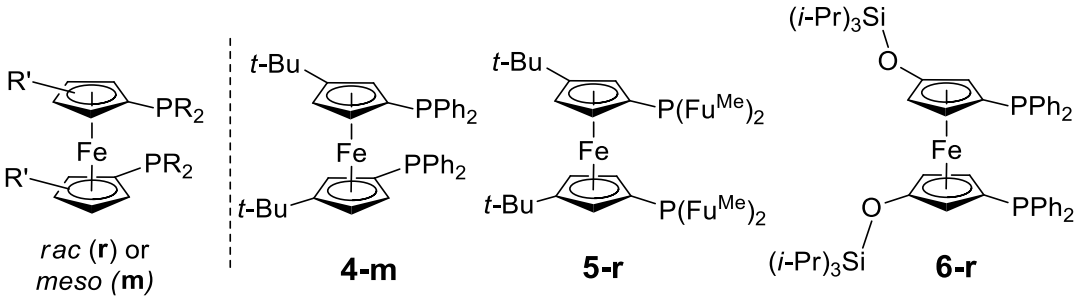

3,3'-Substituted ferrocenyl 1,1'-diphosphines were formed from assembly of appropriately substituted cyclopentadienyl (Cp) lithium salts with iron(II) dichloride.[14c] A mixture of chiral *rac* and achiral *meso* diastereomers was obtained, which can be separated by fractional crystallization and chromatography. We investigated the coordination to Au(I) of the diphosphine **4-m** (Chart 2) and **4-r**. These diphosphines are structurally different from dppf because of the restricted rotation around the iron center that is due to the presence of *tert*-butyl substituents on the Cp rings. The reaction of 1:1 equivalent of Au(I) with **4-r** resulted in a mixture of compounds that we failed to isolate and characterize. In contrast the reaction of 1:1

equivalent of **4-m** (δ ^{31}P = –20.09) and [AuCl(SMe$_2$)] in CH_2Cl_2 for 5 min at room temperature quantitatively yields a single product **7** (Scheme 1), which was characterized in ^{31}P NMR by an AB signal (δ ^{31}P = 36.5) with an intense $^2J_{PP}$ = 316 Hz.

Scheme 1. Gold(I) Chloride Coordination to Ferrocenyl Diphosphine **4-m**

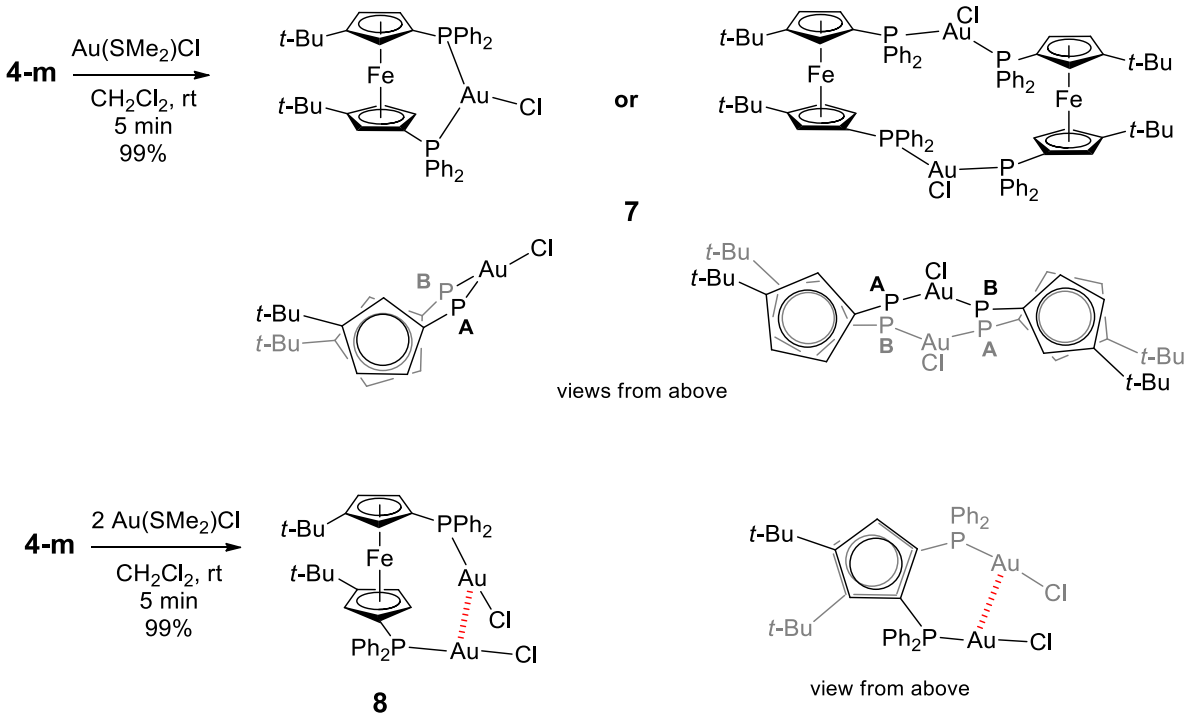

The narrow signal width observed for the AB spin system in ^{31}P NMR led us to exclude the formation of a polymeric adduct for **7** (similar to **1c**, Chart 1). Either mononuclear or dinuclear gold complexes may be hypothesized from the ^{31}P and ^{1}H NMR data (Scheme 1). In related ferrocenyl gold complexes for which X-ray structures have been reported, a single example of 1,1'-mononuclear gold coordination has been reported with a *cis* chelating angle P–Au–P of 116.1(1)° (CCDC name ZAKXEO).[19b] A symmetry plan in which is embed the [P,P–AuCl] fragment led to a singlet resonance in ^{31}P NMR. Concerning dinuclear structures some related

examples of $[Au_2(P,P)_2X_2]$ complexes are known,[20] and this coordination has been suggested for dicationic complexes involving dppf.[17a] However, to the best of our knowledge no X-ray structure has been reported for such digold "locked" pseudo-*trans* coordination. A pseudo-*trans* coordination of [P,P-AuCl] fragments has been reported for polymeric complexes of dppf. In these compounds the P–Au–P angles adopt values ranging from 136.48° to 155.24° (CCDC names PODFOD, WEFXOU, WEFXUA).[18] A resembling AB spin system with $\delta^{31}P = 28.4$, $^2J_{PP} = 309.0$ Hz has been reported recently for a cationic Au^ICl complex *trans*-dicoordinated by $RP(Mesityl)_2$ groups within an unsymmetrical arrangement.[21] Finally, it remains uncertain to relate the ^{31}P NMR signal and strong $^2J_{PP}$ of **7** to either a mononuclear *cis*-chelating or a dinuclear pseudo-*trans* arrangement, while HRMS was found at 863.18945 ($[M\text{-}Cl]^+$) for **7**.

By reacting two equiv of $[AuCl(SMe_2)]$ with **4-m**, complex **8** was obtained (Scheme 1, bottom) and characterized in ^{31}P NMR by a single broad peak resonance at 28.5 ppm. Variable temperature NMR (VT-NMR) highlighted a fluxional behavior for the complex **8**. However, complex **8** is thermodynamically stable and we did not observe any intermolecular exchange process involving **4-m** and **7** (see FIGSI2 in SI). The phosphino groups environment is averaged at 303 K (30 °C) in solution. The broad signal undergoes decoalescence between 0 and –40 °C. At –80 °C two singlets are observed at 25.5 and 30.5 ppm clearly distinguishing two phosphino groups involved in different environment without mutual spin couplings through gold atoms. XRD studies from single crystals of **8** evidenced in the solid state an unsymmetrical dinuclear structure (Figure 1), consistent with the ^{31}P NMR data in solution obtained at –80 °C.

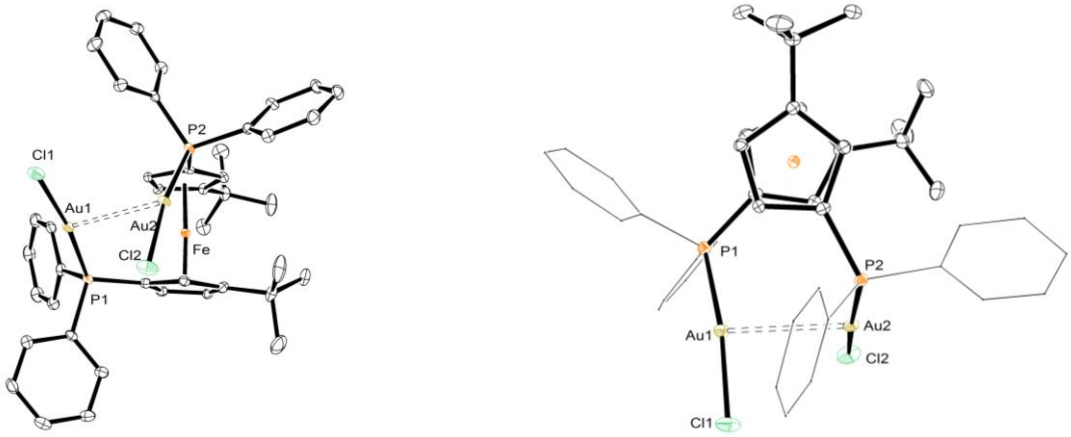

Figure 1. Ortep views of the bis(diphenylphosphino)ferrocene digold(I)chloride complex **8**, left: side view, right: top view. In both view, hydrogen atoms and solvent molecules are omitted for clarity (thermal ellipsoids are drawn at 50% probability level). Selected distances (Å) and angles (°): Au1•••Au2 = 3.0781(6), Au1–P1 = 2.2388(12), Au1–Cl1 = 2.3099(15), Au2-P2 = 2.2287(12), Au2–Cl2 = 2.2961(14), P1–Au1–Cl1 = 172.22(5), P2–Au2–Cl2 = 170.16(5), P1–Ct1–Ct2–P2 = 74.69(6) where Ct1 and Ct2 are the centroids of the Cp rings.

Complex **8** displays an intramolecular aurophilic interaction Au•••Au' = 3.0781(6) Å between its gold(I) centers. Deviation from linearity of the P–Au–Cl angles range between 170-172 °. The structure of diphosphine **4-m** favors the formation of a dinuclear gold (I) chloride complex with aurophilic interactions.

We then examined digold formation using the *rac* diphosphine **5-r** (Chart 2), to assess the effect of changing the phosphino substituents $–PR_2$. Ligand **5-r** bears difurylphosphino groups and was synthesized as a mixture with **5-m**, upon separation less than 5% of **5-m** remains. The digold complex **9** (Scheme 2, $\delta\,^{31}P$ = –17.94) was quantitatively formed from **5-r** ($\delta\,^{31}P$ = –65.41).

Scheme 2. Gold(I) Coordination to Ferrocenyl Diphosphine **5-r**

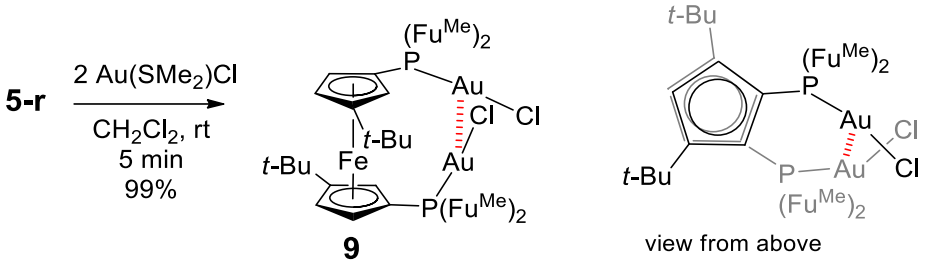

Complex **9** is a dinuclear gold complex also with aurophilic interactions, albeit slightly longer than in **8**: Au•••Au' = 3.2349(6) Å (Figure 2). Accordingly, a deviation from linearity of the P–Au–Cl angles of 171.06(7)° is observed. Complex **9** belong to the C_2 symmetry point group (crystallographic axis). This is a higher symmetry in comparison to **8** that incorporates *meso* diphosphine **4-m**. A structural difference between **8** and **9** is the horizontal and vertical alignment of aurophilic gold atoms, respectively, regarding the centroid(Cp)–Fe–centroid(Cp) axis.

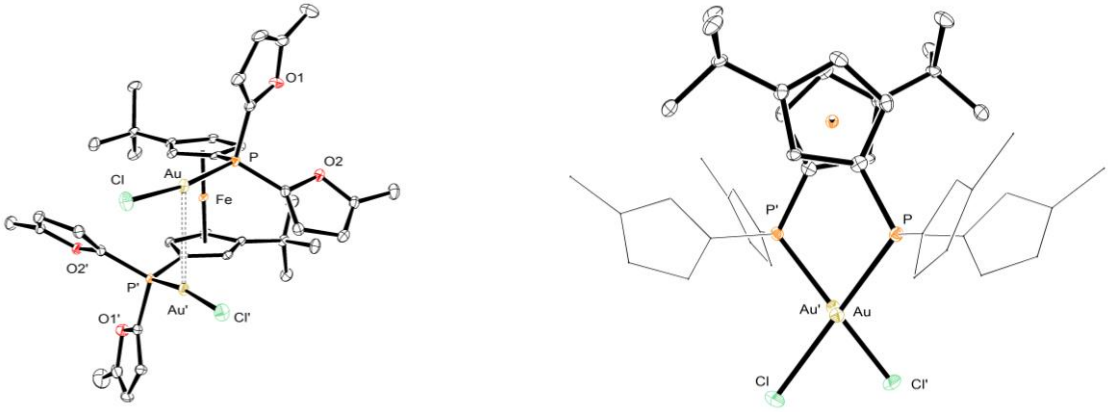

Figure 2. Ortep views of difurylphosphino digold(I) chloride complex **9**, left: side view, right: top view. In both view, hydrogen atoms and solvent molecules are omitted for clarity (thermal ellipsoids are drawn at 50% probability level). Selected distances (Å) and angles (°): Au•••Au' = 3.2349(6), Au–P = 2.2247(17), Au–Cl = 2.2868(19), P–Au–Cl = 171.06(7), P–Ct–Ct'–P' = 54.75(11) where Ct and Ct' are the centroids of the Cp rings. The 'primed' atom names refer to a *C2* crystallographic axis related atoms.

Compared to digold halide complexes incorporating dppf as ligands the presence of *tert*-butyl groups in ferrocenylphosphine ligands appears determining for the formation of aurophilic interactions in complexes **8** and **9**. We thus investigated change of these bulky groups for different steric properties. We synthesized the diphosphine **6-r** (Chart 2, $\delta\,^{31}P = -16.6$) as *rac* stereoisomer for coordination with two equiv of [AuCl(SMe$_2$)]. The new diphosphine **6-r** was obtained in a mixture with its diastereomer **6-m** (50:50, $\delta\,^{31}P = -17.8$). The diphosphines **6** are substituted in 3,3'-position by oxysilane groups –OSi(*i*-Pr)$_3$. Isolation of pure diastereomers could not be successfully achieved. Thus, complex **10** incorporating **6-r** (Scheme 3) was formed together with its analogue incorporating the *meso* diphosphine **6-m**, however upon crystallization **10** was obtained pure.

Scheme 3. Gold(I) Complex **10** of Oxysilane Ferrocenyl Diphosphine **6-r** (from *racemic mixture* ***6-r*** + ***6-m***)

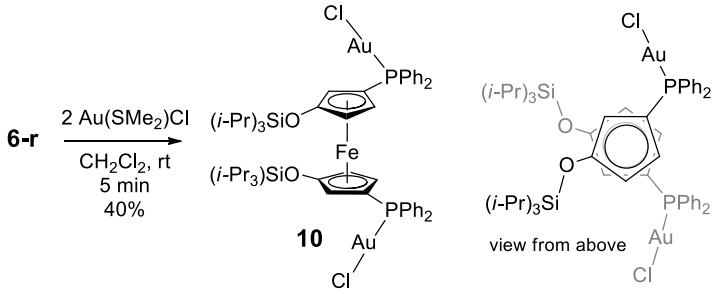

These gold complexes are characterized in ^{31}P NMR by singlets ($\delta\,^{31}P$ = 28.9 and 27.6, respectively). Single crystals of **10** analyzed by X-ray diffraction indicated the formation of a dinuclear gold edifice without gold•••gold interaction contrary to **8** and **9** (Figure 3). The complex **10** belong to the C_2 symmetry point group (crystallographic axis) in which the orientation of the phosphino groups, with large torsion angle P–Ct–Ct'–P' = 119.73(4)°, precludes short contact distances (Au separation > 8.0 Å). Accordingly, the P–Au–Cl angles of 177.21(3)° are close to linearity. The oxygen atom, seen as a spacer, presumably adds a

rotational degree of freedom to the ferrocene backbone in diphosphine **6-r** in comparison to *tert*-butylated diphosphines **4** and **5**. This would explain a lesser steric control exerted by –OSi(*i*-Pr)$_3$ groups in complex **10**.

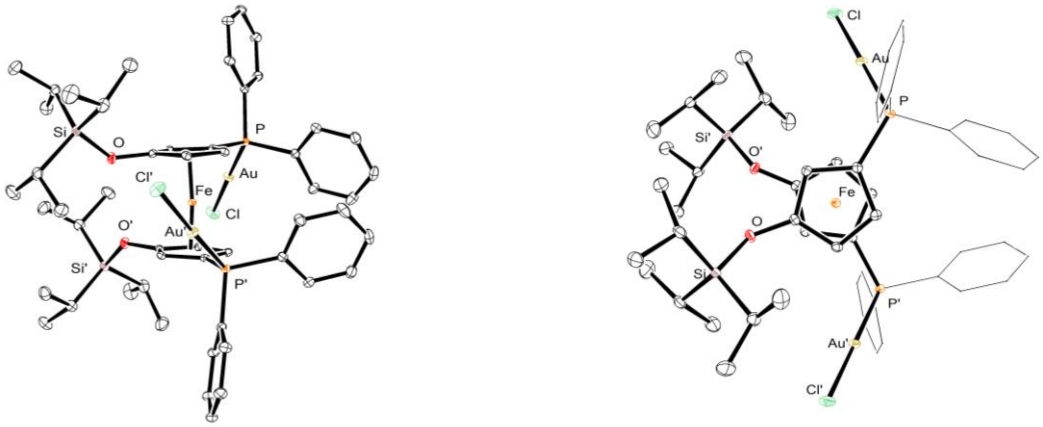

Figure 3. Ortep views of dinuclear gold(I) chloride complex **10**, left: side view, right: top view. Hydrogen atoms are omitted for clarity (thermal ellipsoids are drawn at 50% probability level). Selected bond distances (Å) and angles (°): Au–P = 2.2282(9), Au–Cl = 2.2814(10), P–Au–Cl = 177.35(4), P–Ct–Ct'–P' = 119.73(4) where Ct and Ct' are the centroids of the Cp rings. The 'primed' atom names refer to a *C2* crystallographic axis related atoms.

Considering the new dinuclear gold complexes **8-10** and the literature reports on dppf,[7,17-19] the ferrocenyl diphosphines bearing *t*-Bu groups have a higher propensity to form gold dinuclear aurophilic complexes. We assumed that the sterics provided by *tert*-butyl groups to ferrocene backbone are at the origin of this inclination. Thus, we further explored the formation of polynuclear gold complexes by using the related *tert*-butylated ferrocenyl tetraphosphine **11** (Figure 4) as ligand for coordinating $Au^{I}Cl$.

Gold(I) Complexes of a Congested Ferrocenyl Tetraphosphine. Tetraphosphine **11** is synthesized from the assembly of appropriately substituted lithium cyclopentadienyl salts with $FeCl_2$ (Figure 4).[22] Unclassical large nonbonded ("through-space") nuclear spin coupling $^{TS}J_{AA'}$ of about 60 Hz between the heteroannular phosphorus nuclei A and A' has been studied for **11**.[14a] Nuclei A and A' atoms are magnetically nonequivalent and as such pertains to an AA′BB′ spin system distinguishing central (A,A') and peripheral (B,B') atom pairs (Figure 4, left). The "through-space" coupling constant $^{TS}J_{AA'}$ differs from $^{4}J_{A'B}$, $^{4}J_{AB'}$, and $^{4}J_{BB'}$ which are all null.[14a] X-ray structure analysis of **11** evidences a close distance d(PA···PA') = 3.70 Å related to its conformational rigidity. The resulting P lone-pair overlapping is at the origin of the strong nonbonded $^{TS}J_{AA'}$.

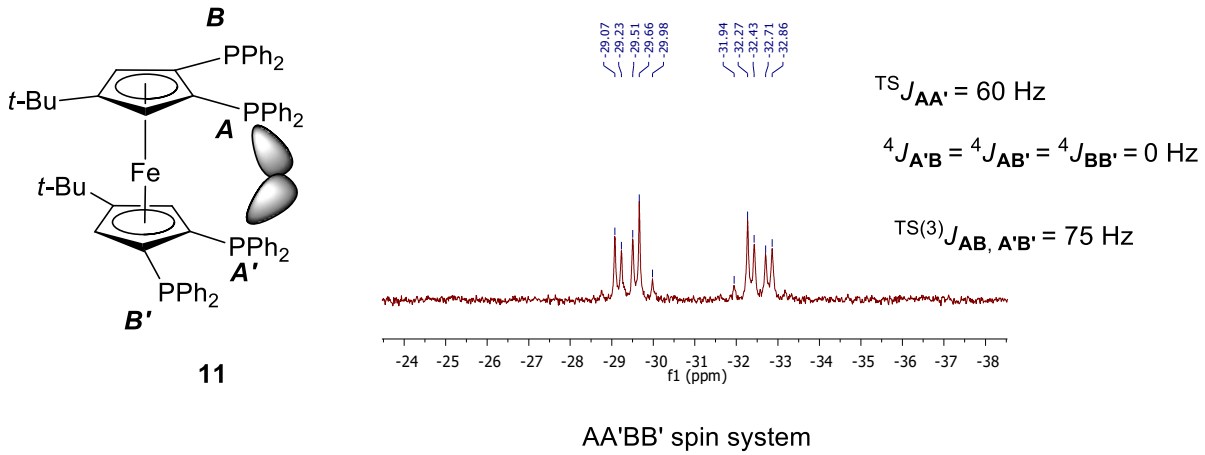

Figure 4. Tetraphosphine **11** with an AA'BB' spin signature (^{31}P NMR, 202.44 MHz, in CD_2Cl_2 at 25 °C). The overlap of lone-pairs from proximal central phosphines (A, A') convey nuclear spin-spin coupling.[23]

Nonbonded spin-spin nuclear coupling transmission mechanism has been studied theoretically.[24-26] Constrained ferrocenyl polyphosphines and their coordination complexes are particularly pertinent tools to investigate this phenomenon because of the close proximity between magnetically inequivalent P-nuclei they can provide.[23, 27, 28]

We investigated the coordination of **11** with various equivalents of $Au^{I}Cl$ salt. Gold(I) complex **12** was quantitatively obtained from reacting **11** with one equiv of $[AuCl(SMe)_2]$ (Figure 5). The ^{31}P NMR spectra of **12** in CD_2Cl_2 shows two triplets centered respectively at $\delta^{31}P$ = 10.4 and –18.5, with $J_{PP'}$ = 54 Hz. This NMR signature indicates a symmetrical complex in which two pairs of phosphorus undergo mutual nuclear spin coupling (Figure 5, top). One phosphorus pair is bonded to a metal center (δ = 10.4), while the other remains uncoordinated ($\delta^{31}P$ = –18.5). ^{31}P NMR analysis achieved at low temperature in CD_2Cl_2 down to –80 °C, and in other deuterated solvents ($CDCl_3$ and C_6D_6) did not reveal significant labile or dynamic behavior for **12** (see FIGSI3). The complex remains stable even at 360 K. This NMR pattern is consistent with two structures either mononuclear or dinuclear (Figure 5). In the high-resolution mass analysis of **12**, a molecular mass signature at m/z = 2498.52852 corresponding to a fragment $[L_2Au_2Cl]^+$ was observed (FIGSI4, *caution: dimerization in the mass process may also occur*).

We simulated the ^{31}P NMR spectra of gold complex **12** (G-NMR, FIGSI5). ^{31}P NMR spectroscopy is consistent with the structures proposed in Figure 5 for a formally AA'XX' spin system simplified to A_2X_2.[29] A null value is obtained for AA' and XX' $J_{PP'}$ couplings while the pseudo A_2X_2 triplet arises from $^3J_{AX} = {}^3J_{A'X'}$ = 54 Hz. Additionally a strong heteroannular ^{31}P nuclei nonbonded coupling $^{TS}J_{X'A} = {}^{TS}J_{XA'}$ also close to 54 Hz is observed. This signature corresponds to a “through-space” nuclear spin coupling transferred via spin polarization of a phosphorus electron lone-pair overlapping with P' electrons involved in a σ(P'–Au) bond.[14a]

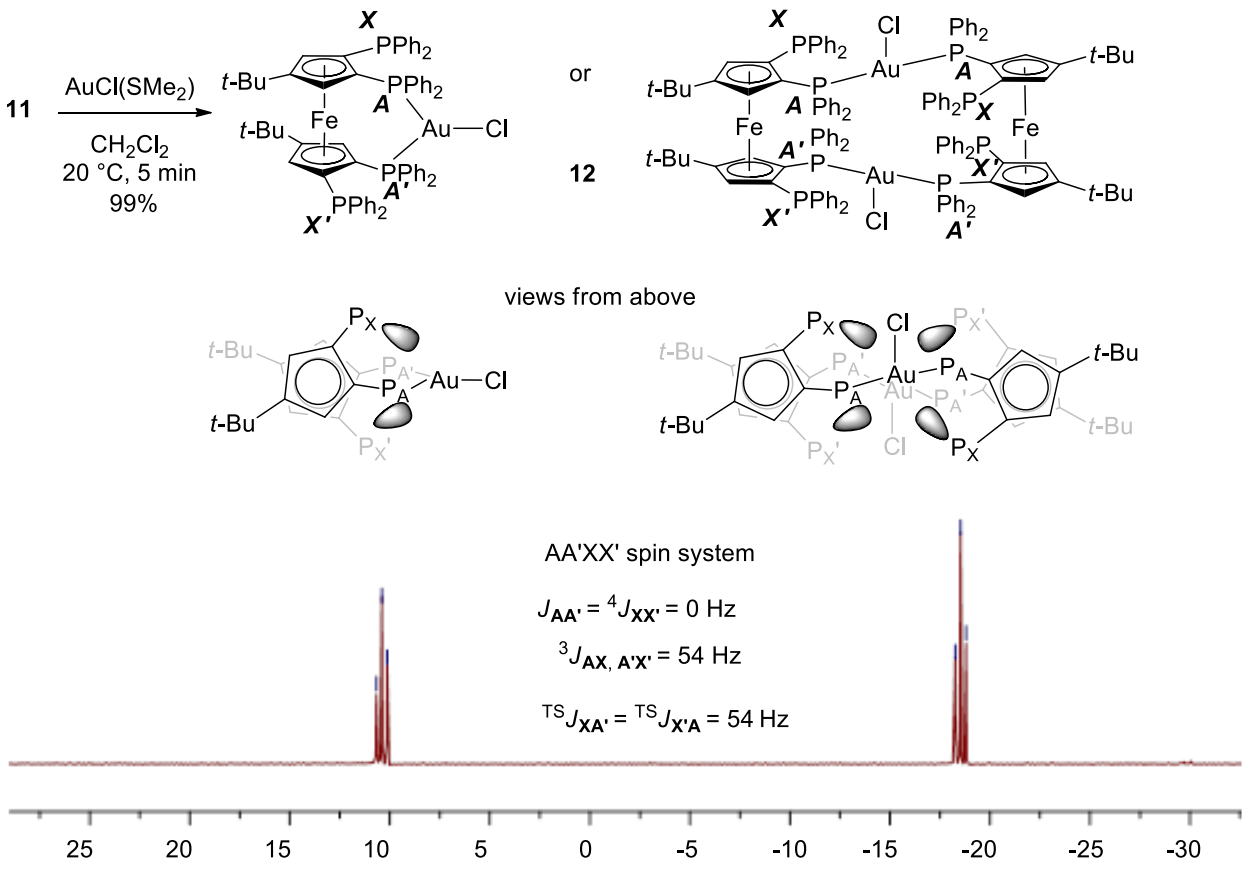

Figure 5. Synthesis of the gold mononuclear complex **12** and ^{31}P NMR in CD_2Cl_2 (25 °C, 202.44 MHz): spin system AA'XX' (pseudo-A_2X_2).

Only a very restricted number of examples of scalar spin coupling constants exist in which nuclear spin-spin coupling is transmitted "through-space" *via* a single lone-pair in interaction with another proximate nuclei involved itself in a covalent bonding.[23] Representative examples were recently reported that are depicted in Chart 3, and which supports $^{TS}J_{X'A} = {}^{TS}J_{XA'} =$ 54 Hz found here for **12**.[14a, 30, 31]

In the complex **a** (Chart 3) the lone-pair of P interacts with a bonding electron-pair shared between P' and the palladium metal center. This situation gives rise to a strong $J_{PP'}$ = 24 Hz.[14] The Jordan group reported with complex **b** a similar $^{31}P^{19}F$ "through-space" *J* coupling arising from the overlap of a fluorine atom lone-pair and a σ(P–Pd) electron-pair.[30] Emslie and co-

workers in complex **c** have observed a "through-space" coupling arising from a nonbonding interaction between the lone-pair on P and the dative bonding electron-pair between P' and Al, this three-center interaction is characterized by a strong $J_{PP'}$ = 31 Hz.[31]

Chart 3. (P, P) and (P, F) "through-space" coupling involving three-centers: a lone-pair and a bonding electron-pair to metal (Pd and Al).

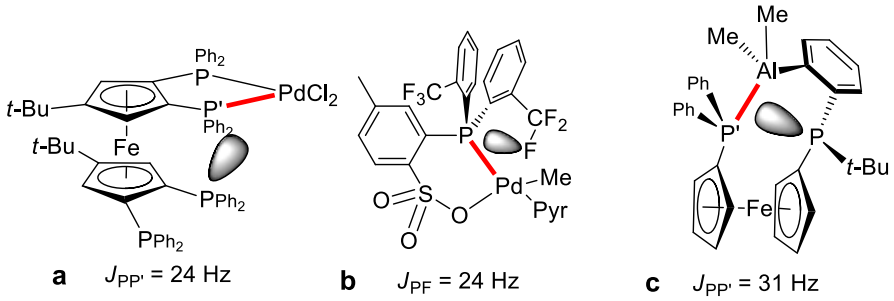

Thus, in gold complex **12** the coupling between uncoordinated P nuclei (δ = –18.5) and P' nuclei coordinated to gold (δ = 10.4) corresponds to this kind of three-center interactions. The strong $J_{PP'}$ = 54 Hz is consistent with the larger extent of gold valence orbitals (compared to Pd and Al in the reported examples in Chart 3) and certainly does not fit common $^{3}J_{PP'}$ or $^{4}J_{PP'}$.[23]

In the solid state, an unsymmetrical mononuclear structure was solved for **12** by XRD (Figure 6). The gold center was found tricoordinated with its AuCl fragment located proximate to the isosceles triangle formed by P1, P2, and P1'. One of the (P,Au) distances is longer that the others (P2–Au = 2.3499(15) Å, P1'–Au = 2.3261(17) Å and P1···Au = 2.7451(16) Å) excluding a tetracoordination of Au. The sum of the angles formed at gold atom involving P1', P2 and Cl nuclei equal 358.41(10)°. In the structures reported for tetrahedral complexes of the type [ClAuP$_3$],[32] the three Au–P bonds are found similar with a mean value of 2.375 Å (±0.031 Å for 36 observations from CCDC).[33] A significant residual peak was found in the structure refinement

that is associated to Au. This was modelled by a second position for the gold center (occupancy factor of 10%) bonded to P1 and P1' instead of P2 and P1'. The major unsymmetrical structure is not fully consistent with solution NMR. Yet, the multinuclear solution NMR recorded after redissolution from the single crystals was found unchanged, showing that in solution the symmetrical configuration dominates.

The proximity of the third phosphorus atom P1 to the (P2, P1')–Au–Cl fragment observed in the X-ray structure is supportive of "through-space" $J_{PP'}$ couplings previously assumed in ^{31}P NMR solution. For this, however, an appropriate orientation of P_X lone-pair is needed, allowing interaction with the Au–$P_{A'}$ bond and resulting in the P_AP_X spin couplings.

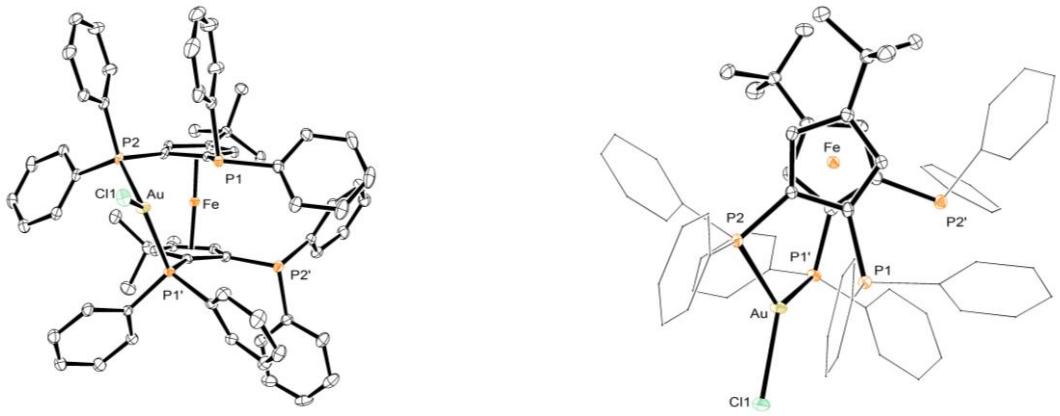

Figure 6. Ortep views of mononuclear gold(I) chloride complex **12**, left: side view, right: top view. In both view, hydrogen atoms and solvent molecules are omitted for clarity (thermal ellipsoids are drawn at 50% probability level). Selected bond distances (Å) and angles (°): P1···Au = 2.7451(16), P2–Au = 2.3499(15), P1'–Au = 2.3261(17), P2–Au–P1' = 113.19(6), P2–Au–Cl1 = 120.21, P1'–Au–Cl1 = 125.01(6).

In order to visualize the direction of lone-pair of P1 in compound **12**, we resorted to the topological analysis of the electron localization function (ELF) based on density functional theory (DFT) calculations. The ELF function can be interpreted as a signature of the electronic-pair distribution, split into an intuitive chemical picture: core, bonding and nonbonding region

pairs (the so-called basins). The lone-pair of P1 is shown on Figure 7, which clearly confirmed the close proximity of P1 lone-pair and its adequate directionality regarding the gold coordination area.

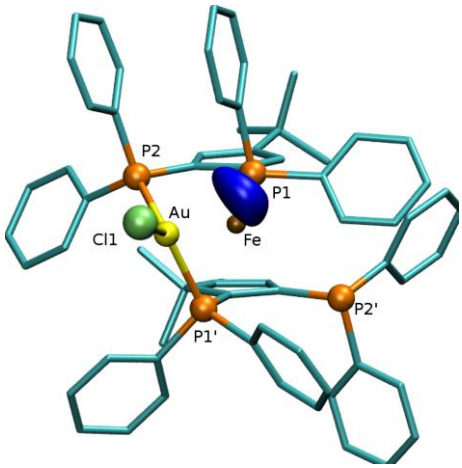

Figure 7: Nonbonding ELF region for the P1 phosphorus in compound **12** (Fe in ochre, C in cyan, Au in yellow, Cl in lime, P in orange, hydrogen atoms are omitted for clarity; ELF Isovalue = 0.8).

Tetraphosphine **11** was reacted with three equivalents of [AuCl(SMe_2)]] to give complex **13** (Figure 8) which was isolated in 33% yield from a complex mixture of species. The ^{31}P NMR in solution is in agreement with an AA'BB' spin system (δ ^{31}P = 19.31, 18.91) showing nuclear spin couplings $J_{AA'}$ and $J_{BB'}$ = 0 Hz, and J_{AB} = $J_{A'B'}$ = 12 Hz and $J_{A'B}$ = $J_{AB'}$ = 12 Hz, as suggested by NMR simulation (FIGSI6). In trinuclear complex **13** $J_{A'B}$ and $J_{AB'}$ coupling constants are most probably conventional long-range ^4J, and accordingly their value (12 Hz) is much lower than the more direct "through-space" couplings found in mononuclear **12** (54 Hz) and relaying on lone-pair availability.

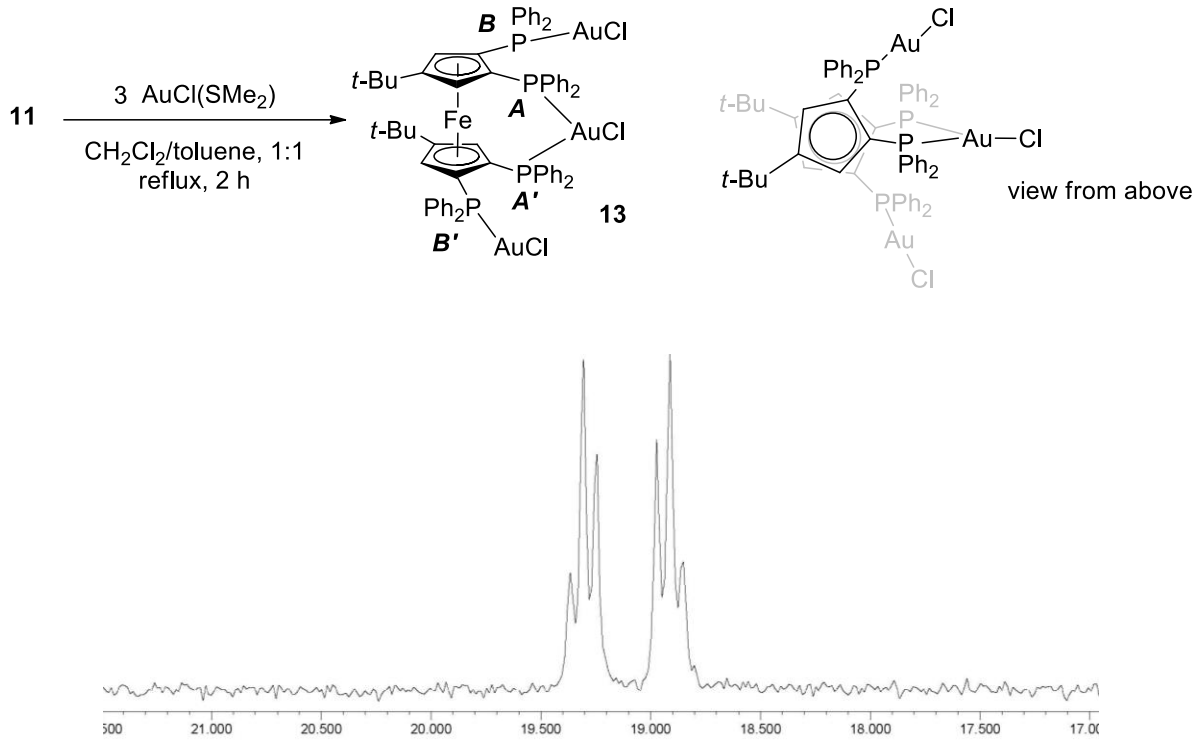

Figure 8. Trinuclear gold complex **13** and ^{31}P NMR in CD_2Cl_2 (25 °C, 202.44 MHz).

X-ray diffraction structure for complex **13** confirmed in the solid state the coordination sphere around the gold centers that was proposed from NMR data (Figure 9). In addition, complex **13** displays fairly short intramolecular gold–gold distances from which one fall in the range of aurophilic interactions Au1•••Au2 = 3.2745(5) Å, while the other distance is longer Au2...Au3 = 3.5784(7) Å (van der Waals radii < 1.7 Å).

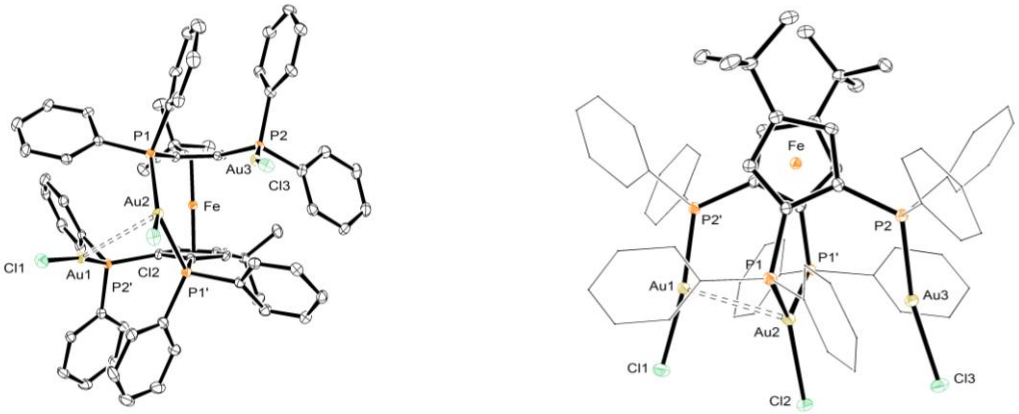

Figure 9. Ortep views of trinuclear gold(I) **13**, left: side view, right: top view. In both view, hydrogen atoms and solvent molecules are omitted for clarity (thermal ellipsoids are drawn at 50% probability level). Selected bond distances (Å) and angles (°): Au1•••Au2 = 3.2745(5), Au2…Au3 = 3.5784(7), P2'–Au1 = 2.2356(19), Au1–Cl1 = 2.3080(21), P1–Au2 = 2.2777(19), P1'–Au2 = 2.4006(20), Au2–Cl2 = 2.4532(22), P2–Au3 = 2.2285(19), Au3–Cl3 2.3000(21), P2'–Au1–Cl1: 168.80(7), P1–Au2–P1' = 119.00(7), P1–Au2–Cl2 = 135.69(7), P1'–Au2–Cl2 = 104.48(7), P2–Au3–Cl3 = 166.84(7).

The attractive influence of the central gold atom on the two lateral gold atoms is marked by P–Au–Cl and P'–Au–Cl bond angles which strongly deviate from linearity (168.80(7)° and 166.84(7)°, respectively). The modest 0.3 Å difference between the atom separation for (Au1, Au2) and (Au2, Au3) pairs suggests that in solution their mutual positions may be inverted. This is possibly at the origin of the fairly broad appearance of AA'BB' ^{31}P NMR multiplets, which is not significantly modified upon VT measurement between –80 to 130 °C. The molecular structure of **13** is a unique example of a dissymmetric aurophilic interaction involving a formally 14e$^-$ gold(I) and a 16e$^-$ gold(I).

From the reaction of **11** with larger amount of gold salt [AuCl(SMe$_2$)] (4 to 6 equiv), complex **13** only was repeatedly obtained at rt or at reflux in toluene, evidencing its thermodynamic stability.

The reaction of **11** with two equiv. of [AuCl(SMe_2)] provided a mixture of three products in roughly equivalent amount (Figure 10). Two of them were easily identified as being the 1:1 [tetraphosphine/gold] complex **12** and the 1:3 [tetraphosphine/gold] complex **13**. Two additional signals at 20.4 ppm and –5.8 ppm were identified as coming from a single compound **14**, as confirmed by ^{31}P-^{31}P 2D correlation NMR. The very broad resonance and middle range chemical shift at –5.8 ppm suggested a dynamic behavior for complex **14**. Therefore, ^{31}P NMR of the entire system was studied at variable temperature between –80 °C and 130 °C in a mixture of 50:50 DMF/CD_2Cl_2 (Figure 11).

Mononuclear gold complex **12** and trinuclear gold complex **13**, which are present in the mixture show only little chemical shifts modification in the VT-NMR experiments. In the range –80 °C to 130 °C these minor changes are not involving dynamic coordination/decoordination of phosphorus donors, since the signals remain located in the same area: 10/15 ppm and –18/–23 ppm for **12**, and 19 ppm for **13**, without coalescence/decoalescence phenomenon. Conversely, the additional signals attributed to **14** clearly show decoalescence between 130 °C and –80 °C shifting from around 20 and –5 ppm, to around 25 and –35 ppm, see Figure 11. Thus, the dynamic phenomenon involving **14** is clearly intramolecular and is not due to dissociative/intermolecular mechanism between **12**, **13** and **14**.

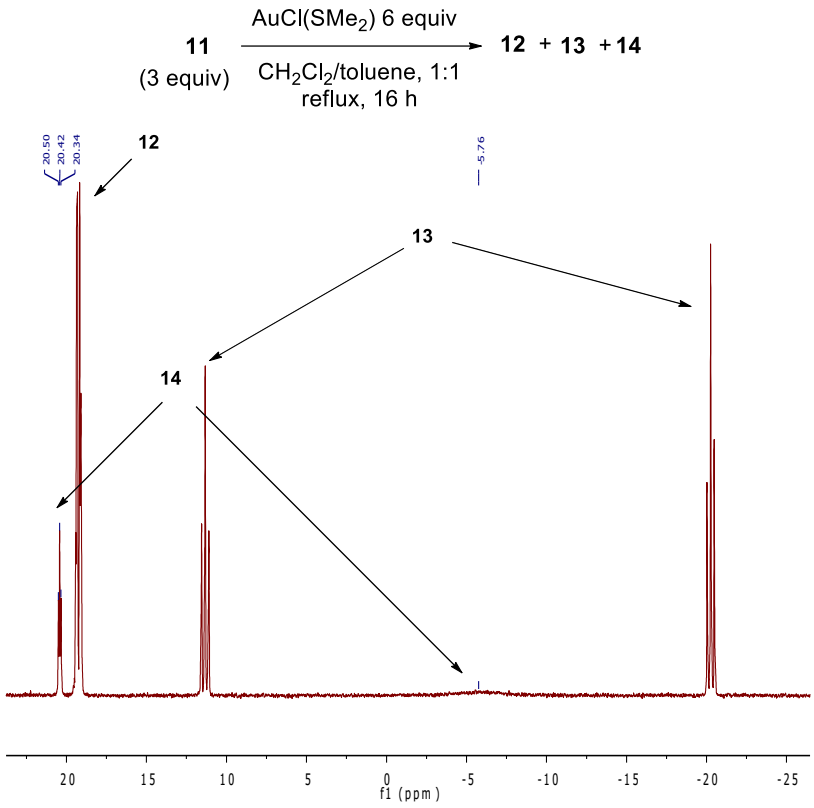

Figure 10. ^{31}P NMR in CD_2Cl_2 (25 °C, 202.44 MHz) of complexes **12-14**.

More specifically, the signals attributed to species **14** at $\delta^{31}P$ = 20.4 and –5.8 (between 27 °C and 47 °C) undergo a coalescence phenomenon upon cooling, and these signals fully disappear at –13 °C. The signals decoalescence is observed around –33 °C and gives rise between –53 °C and –80 °C to a set of new signals at higher and lower fields: around –35 ppm and 25 ppm. At –80 °C the dynamic behavior is frozen to give from the broad signals at 20.4 ppm and –5.8 ppm a strong signal at –35 ppm that is associated to new signals at 22 and 27 ppm; the correlation between these signals was established by 2D COSY NMR $^{31}P\{^1H\}$-$^{31}P\{^1H\}$ achieved at 67 °C and –80 °C. Thus, at low temperature **14** incorporates both coordinated and pendant phosphino groups, which are involved in dynamic exchange above –53 °C.

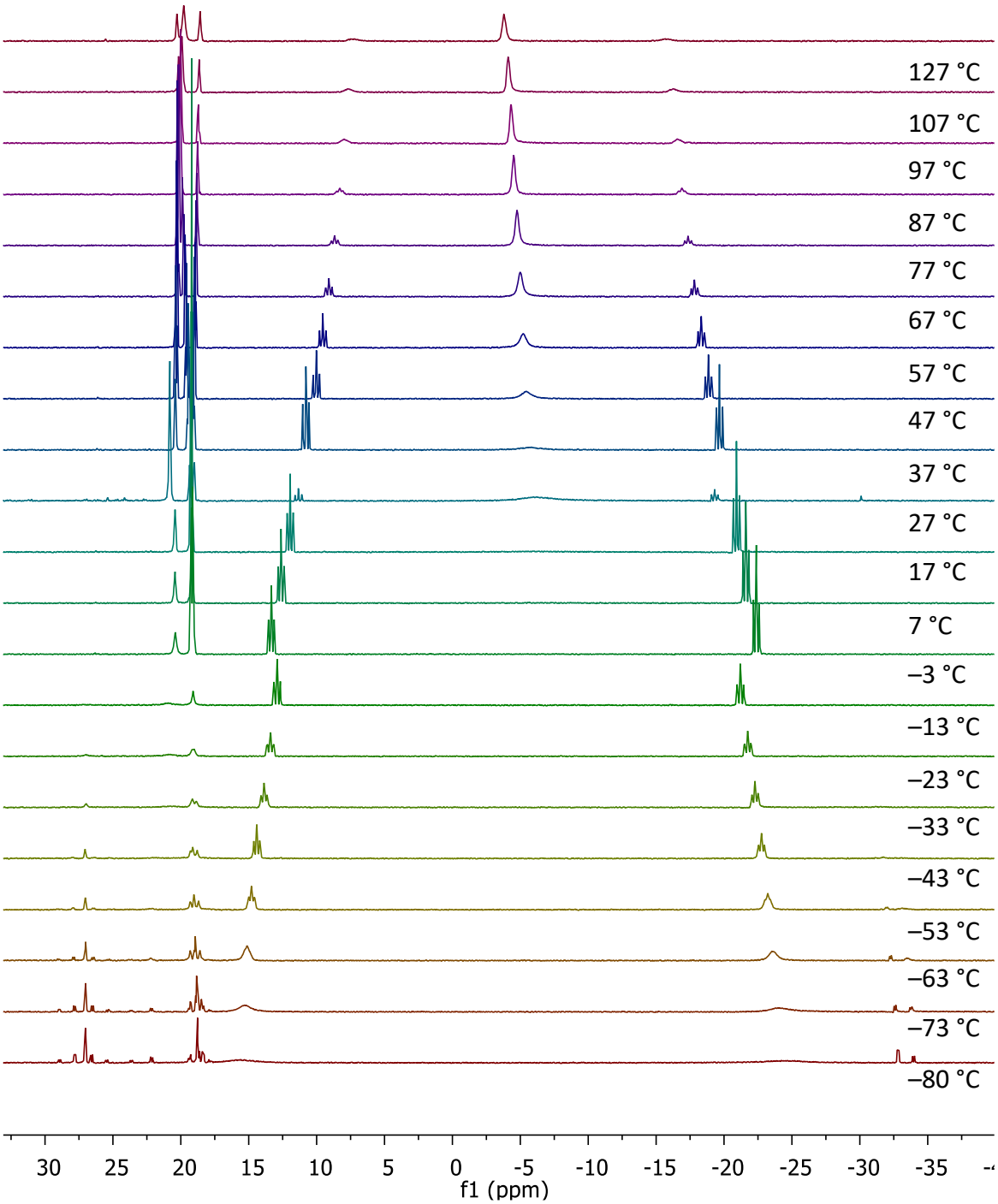

Figure 11. VT-^{31}P NMR in DMF/CD_2Cl_2 (–80 °C to 127 °C, 202.44 MHz).

To further elucidate the structure and dynamic behavior of **14** we successfully grew single crystals from the mixture obtained in CH_2Cl_2 by pentane diffusion. A dinuclear gold complex

was obtained, different from mononuclear **12** and trinuclear **13**, and adequately fitting the global stoichiometry of the reaction (Figure 10, top); it was analyzed by XRD (Figure 12).

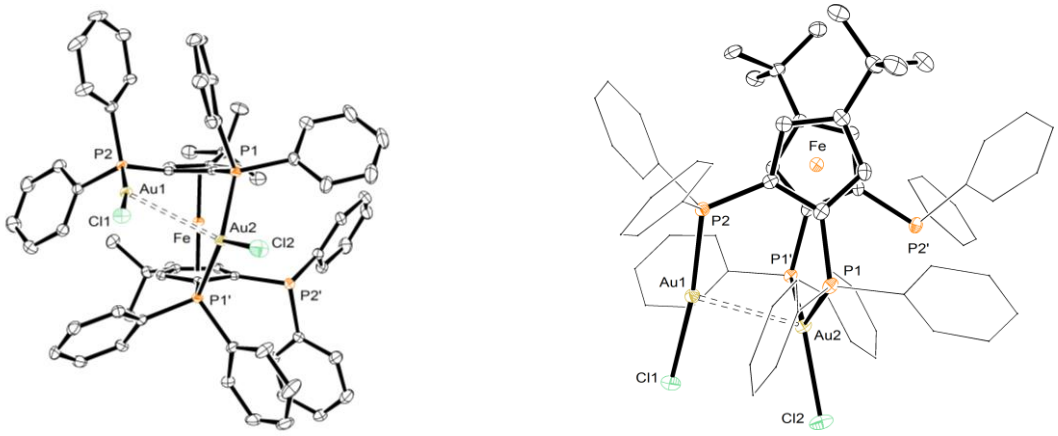

Figure 12. Ortep views of dinuclear gold(I) **14**, left: side view, right: top view. In both view, hydrogen atoms and solvent molecules are omitted for clarity (thermal ellipsoids are drawn at 50% probability level). Selected bond distances (Å) and angles (°): Au1•••Au2 = 3.1436(6), P2–Au1 = 2.2318(13), Au1–Cl1 = 2.2993(14), P1–Au2 = 2.3305(12), P1'–Au2 = 2.2931(12), Au2–Cl2 = 2.4720(15), P2–Au1–Cl1: 171.62(5), P1–Au2–P1' = 119.29(5), P1–Au2–Cl2 = 112.51(5), P1'–Au2–Cl2 = 125.29(5).

In complex **14** the two gold centers Au1 and Au2 are embedded in different environment: Au1 is dicoordinated in a formally 14e$^-$ complex with a linear geometry. The Au2 atom is tricoordinated in a formally 16e$^-$ complex with a trigonal planar geometry. The dinuclear complex **14** displays an aurophilic interaction Au1•••Au2 = 3.1436(6) Å. The crystal structure is slightly disordered: a third Au–Cl group can be found linked to the last phosphorus (occupancy factor of 11%), leading to a structure similar to that of the complex **13**, and indicative of the "filiation" of these complexes. Upon redissolution of the single crystals at the origin of XRD analysis, unexpectedly the 1:1:1 original mixture of complexes **12, 13** and **14** was back obtained, giving solution NMR identical to the ones described above (Figure 10).[34]

DFT calculations were conducted to establish ELF analysis based on the X-Ray structure of complex **14** (Figure 13). For this complex, pendant phosphorus (in blue) and bonded P–Au basins (in pink) were investigated. Unsurprisingly, this decomposition of the phosphorus bonding scheme illustrates the dissymmetry of the two gold centers, confirming that Au1 is involved in one Au–P bond only while Au2 is a tricoordinate complex involved in two Au–P bonds. For complex **14** also the lone-pair of pendant P2' is unambiguously pointing towards Au centers area, a directionality expected to favor intramolecular fluxional behavior.

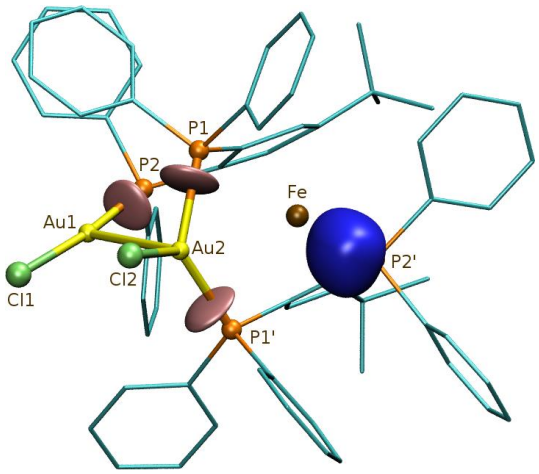

Figure 13. Nonbonding and ELF region for the P2' phosphorus (blue basin) and bonding Au–P regions (pink basins) in compound **14** (Fe in ochre, C in cyan, Au in yellow, Cl in lime, P in orange, hydrogen atoms are omitted for clarity; ELF Isovalue = 0.8).

We finally analyzed NMR spectra of the **12**, **13** and **14** mixture at –80 °C in pure CD_2Cl_2, which gives a consistent attribution of the signals relating to P1, P1', P2 and P2' in the digold complex **14** (FIGSI7 and Figure 14). ^{31}P NMR of the uncoordinated P2' gives a resonance doublet centered at –33.9 ppm with a J_{PP} = 29.3 Hz corresponding to a spin coupling with the doublet at 22.1 ppm found for P1' (J_{PP} = 29.5 Hz). P1 gives rise to the doublet resonances

centered at 23.6 ppm (J_{PP} = 30.1 Hz) and P2 to a signal at 17.8 ppm (J_{PP} = 30.8 Hz). Upon heating, these four signals changed and average to give at 127 °C, as previously seen (Fig. 11), two broad signals located at 19.8 ppm and –3.8 ppm. This signature is explained by the dynamic behavior depicted in Figure 14.

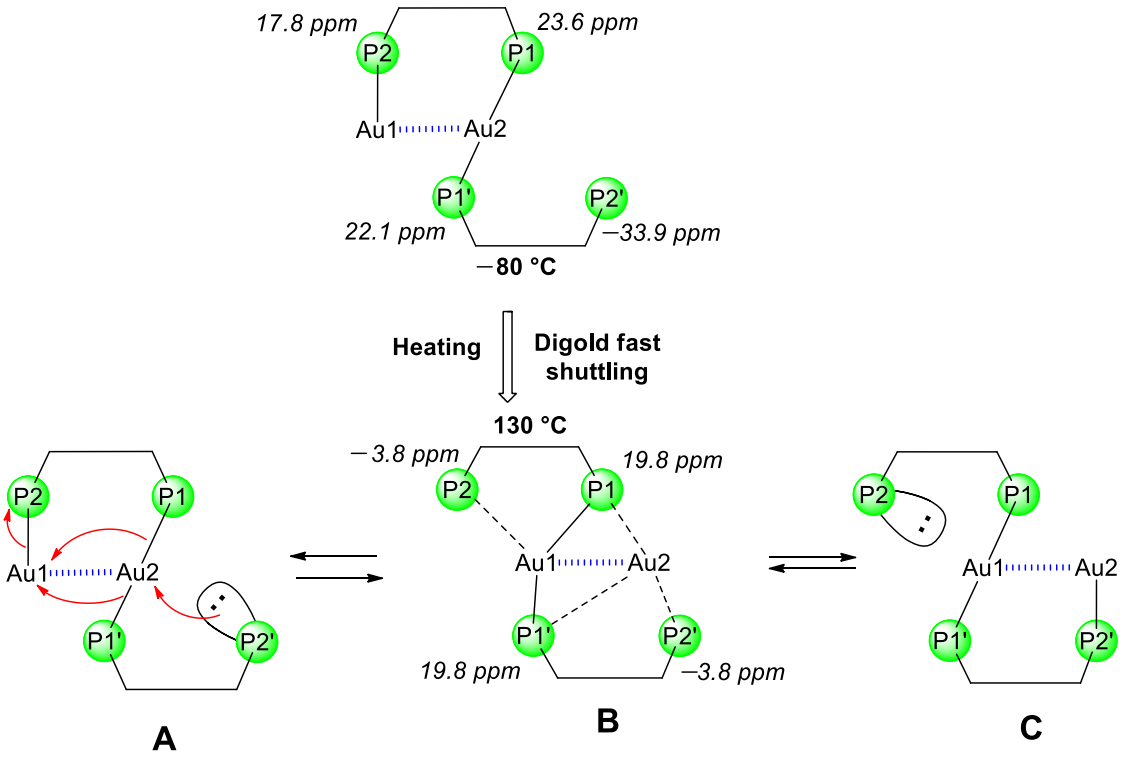

Figure 14. Temperature-dependent dynamic exchange within dinuclear gold complex **14**.

^{31}P NMR at –80 °C is consistent with four different signals for phosphorus (top). Upon heating up to 130 °C, the two broad signals obtained correspond to two different pairs of phosphorus atoms: the peripheral phosphorus P2 and P2', for which the average signal at –3.8 ppm indicates a phenomenon of coordination/decoordination to gold center. In contrast, the central phosphorus P1 and P1' with resonances at 19.8 ppm remains coordinated to a gold center (Au1 or Au2) along the process. Such a process is only possible if a concerted shuttling of digold

aurophilic moiety is operating as depicted in Figure 14. From configuration **A** the lone-pair of P2' coordinates Au2 and induces the decoordination of P1 and P1' from Au2. The P1' and P1 atoms can then coordinate Au1, and induce decoordination of P2, resulting in structure **C** similar to **A** (*via* intermediate **B**). This process is supported by the X-ray structure determined for the digold complex **14** which then corresponds to the extreme situations **A** and **C** (fitting nicely as well the ELF localization and orientation of the P2' lone-pair, Figure 13). Following this hypothesis, the mutual environment of gold centers should remain mostly unchanged since phosphine signals are not differentiated at higher temperature. This indicates a conservation of the dinuclear framework as such, and the Au···Au aurophilic interaction unchanged in the process. This process constitutes a unique dynamic shuttling of aurophilic digold(I) edifice between four phosphorus donors. To a certain extent, this dynamic behavior may be related to the dynamic "oschelating" process occurring without dissociation of the metal–phosphorus bonds and reported in palladium and gold chemistry of *trans*-chelator diphosphines,[35] with in the present case the additional particularity of M···M aurophilic interaction.

CONCLUSION

The introduction of hindering *tert*-butyl groups on the cyclopentadienyl rings of bis(phosphino)ferrocene compounds induces a steric control of the metallocene backbone conformation that is profitable for generating digold(I) halide aurophilic complexes. Previously, dppf analogous gold(I) halide complexes were found to form polymeric compounds or digold molecular complexes with long range Au/Au separation, which precluded aurophilic interaction to form. Thus, this steric control may be a first entrance to actively generate aurophilic gold edifices. This finding was confirmed by generating polynuclear gold species stabilized by a

parent *tert*-butylated tetrakis(phosphino)ferrocene even more congested than bis(phosphino)ferrocenes. Access to mono-, di- and trinuclear gold chloride complexes was achieved that generates previously unseen species in which $14e^-$ and $16e^-$ gold centers co-exist, and are additionally involved in the transmission of nonbonded ("through-space") $^{31}P–^{31}P$ nuclear spin couplings. Only a limited number of examples of resembling scalar spin coupling constants has been reported, in which nuclear spin coupling transmission is supported "through-space" by the lone-pair of one spin active nuclei (P) interacting with another nuclei (P') involved in a covalent bonding (Au). Finally, a dinuclear aurophilic complex supported by the congested *tert*-butylated ferrocenyltetraphosphine was found to display a dynamic behavior in which a concerted shuttling of a dinuclear [ClAu•••AuCl] fragment between the four phosphorus donors of the ferrocenyl tetraphosphine was evidenced by VT-NMR. Further works will aim at taking profit of close proximity in these various digold fragments for concerted catalytic applications.

EXPERIMENTAL SECTION

General Conditions

All reagents were purchased from commercial suppliers and used without further purifications. Reactions were carried out in an atmosphere of argon by means of conventional Schlenk techniques. Solvents were dried and deoxygenated before distillation from sodium benzophenone ketyl. ^1H (300 MHz), ^{13}C (75 or 125 MHz) spectra were recorded on Bruker AVANCE III instrument in $CDCl_3$ solutions. Chemical shifts are reported in ppm relative to $CDCl_3$ (^1H: 7.26 and ^{13}C: 77.16) and coupling constants *J* are given in Hz. High resolution mass spectra (HRMS) were obtained on a Thermo LTQ-Orbitrap XL with ESI source. Flash chromatography was performed on silica gel (230-400 mesh). Preliminary measurement of fluorescence on the gold aurophilic polynuclear complexes indicated that this phenomenon may be mostly quenched by ferrocene.

Computational details

Topological analysis of the electron localization function (ELF)[36] based on density functional theory (DFT) calculations were achieved. These ELF regions match closely the domains of the VSEPR model.[37] Quantum mechanics calculations were performed with the Gaussian09 software package.[38] Geometries were taken directly form the X-Ray data. The electronic density was computed by density functional theory with the B3LYP hybrid

exchange-correlation functional,[39] and developed on the DZP basis set for the gold atom,[40] def2-SVPD basis set for the iron atom[41] and the 6-31+G(d,p) basis set for other atoms.[42] The DZP and def2-SVPD basis sets were taken from the EMSL Basis Set Exchange Web site (*https://bse.pnl.gov/bse/portal; September 7th 2016*). All the topological analyses were carried out from a Kohn–Sham wave function with the TopMoD package.[36c] The ELF isosurfaces were visualized by using the VMD software.[43]

Synthesis of *meso*-1,1'-bis(diphenylphosphino)-3,3′-di-*tert*-butyl ferrocene (4-m). This compound was synthesized according to literature report.[44]

Synthesis of *rac*-1,1′-bis[di(5-methyl-2-furyl)phosphino]-3,3′-di-*tert*-butyl ferrocene (5-r). Iron(II) dichloride (225 mg, 1.78 mmol) was dissolved in THF (20 ml). Lithium (1-(*tert*-butyl)-3-bis(5-methylfuran-2-yl)phosphino]cyclopentadienide (1.14 g, 3.56 mmol) was dissolved in THF (20 mL) in a different flask and was cooled to –40 °C. The solution of the lithium salt was transferred to the suspension of $FeCl_2$. The mixture was allowed to warm to room temperature overnight and was stirred under reflux for further 2 hours. The solvent was removed under vacuum and the residue was filtrated with ether to afford an orange solid as a 7:3 mixture of *rac* and *meso* **5** diastereomers (total yield 75%, 914 mg, 1.34 mmol) which can be separated by chromatography on silica gel (heptane/ether 90/10%). **5-r** yield 50% (610 mg). HR-MS (ESI_{pos}, DCM/MeOH, m/z): calc. $C_{38}H_{44}FeO_4P_2^+$ $[M]^+$ 682.55780, found 682.20697. Anal. Calcd.: C, 66.87; H, 6.50; Found: C, 66.09; H, 6.67. ^{1}H NMR ($CDCl_3$, 300 MHz): δ 1.10 (s, 18H, *t*Bu), 2.26 (s, 6H, *Me*Fu), 2.36 (s, 6H, *Me*Fu), 3.97 (m, 2H, Cp), 4.07 (m, 2H, Cp), 4.29 (m, 2H, Cp), 5.88 (m, 2H, *H*Fu), 6.02 (m, 2H, *H*Fu), 6.28 (m, 2H, *H*Fu), 6.81 (m, 2H, *H*Fu). ^{13}C{^{1}H}($CDCl_3$, 75 MHz): δ 14.1 (s, *Me*Fu), 14.2 (s, *Me*Fu), 30.6 (s, *C*(*t*Bu)), 31.7 (s, *Me*(*t*Bu)), 69.4 (s, Cp), 72.2 (s, Cp), 72.7 (m, Cp), 72.9 (t, $^3J_{CP}$ = 18.16 Hz, Cp), 105.3 (t, $^3J_{CP}$ = 3.96 Hz, *C4*Fu), 106.8 (m, *C4*Fu), 107.0 (t, $^3J_{CP}$ = 3.96 Hz, *C4*Fu), 107.2 (d, $^2J_{CP}$ = 5.7 Hz, *C3*Fu), 119.3 (t, $^2J_{CP}$ = 15.3 Hz, *C3*Fu), 122.2 (d, $^2J_{CP}$ = 2.5 Hz, *C3*Fu), 122.7 (t, $^2J_{CP}$ = 8.3 Hz, *C3*Fu), 150.2 (d, $^1J_{CP}$ = 6.88 Hz, *C2*Fu), 150.3 (d, $^1J_{CP}$ = 6.88 Hz, *C2*Fu), 152.2 (m, *C2*Fu), 156.21 (t, $^4J_{CP}$ = 1.5 Hz, *C5*Fu), 156.8 (m, *C5*Fu). ^{31}P{^{1}H}($CDCl_3$, 121.5 MHz): –65.3.

Synthesis of 1,1'-bis(diphenylphosphino)-3,3'-(tri-*iso*-propylsilyloxy) ferrocene (6). This compound was synthesized by assembly appropriately substituted cyclopentadienes with iron chloride. *Tri-iso-propylsilyloxycyclopentadiene.* Triethylamine (2.3 g, 3.18 ml, 22.8 mmol) and 2-cyclopenten-1-one (1.3 g, 1.4 ml, 16.3 mmol) were dissolved in 50 ml of pentane. Tri-*iso*-propylsilyl trifluoromethanesulfonate (4.3 g, 3.8 ml, 14.1 mmol) was added at room temperature for 15 min. Two phases were formed, the upper one being colorless, while the bottom one being yellow. Stirring was stopped and the upper phase was transferred into a new flask. The solvent was removed *in vacuo* and the product was formed as slightly yellow oil and was quickly used without further manipulation (yield 3.45 g, 14.5 mmol, 89 %). *Caution:* This substituted diene undergoes Diels-Alder reactions and cannot be easily stored it should be freshly prepared and quickly used.

Lithium tri-iso-propylsilyloxycyclopentadienide. Tri-*iso*-propylsilyloxycyclopentadiene (6.6 g, 27.6 mmol) was dissolved in 20 ml THF and the solution was cooled to –80 °C. 1.1 equiv of *n*-butyllithium was added and the mixture was allowed to warm to room temperature overnight. The solvent was removed *in vacuo* and 20 ml pentane was added. The suspension was filtered, washed with 20 ml pentane and dried *in vacuo.* The product (yield 4.36 g, 17.8 mmol, 65 %) was directly used for further phosphination. ^{1}H NMR (THF-d_8, 300 MHz): δ 0.95-0.97 (d, 18H,

CH*Me*$_2$), 1.00-1.12 (sept, 3H, C*H*Me$_2$), 5.07-5.15 (m, 4H, Cp-*H*). ^{13}C NMR (THF-d$_8$, 75 MHz): δ 11.9 (CH*Me*$_2$), 16.9 (*C*HMe$_2$), 90.7 (α-Cp), 95.9 (β-Cp), 138.8 (ipso-C).

Lithium [(1-tri-iso-propylsilyloxy)-3-diphenylphosphino]cyclopentadienide. Lithium tri-*iso*-propylsilyloxycyclopentadienide (4.36 g, 17.8 mmol) was dissolved in THF (30 ml) and cooled to –80 °C. Diphenylphosphine (3.9 g, 3.3 ml, 17.8 mmol) was added. After stirring overnight, the mixture was allowed to warm to room temperature. The solvent was removed *in vacuo* and the residue was suspended in toluene (30 ml) and the mixture was filtered. The filtrate was cooled to –80 °C and *n*-butyllithium (11.2 ml, 17.8 mmol) was added. The mixture was allowed to warm to room temperature overnight. The solvent was removed *in vacuo* and pentane (30 ml) was added. The suspension was filtered and the remaining solid was washed with pentane (20 ml) and dried *in vacuo (*yield, 5.6 g, 13.0 mmol, 73 %). ^{1}H NMR (THF-d$_8$, 600 MHz): δ 1.18-1.19 (d, 18H, CH*Me*$_2$), 1.27-1.33 (sept, 3H, C*H*Me$_2$), 5.46 (m, 1H, Cp-*H*), 5.55 (m, 1H, Cp-*H*), 5.82 (m, 1H, Cp-*H*), 7.16-7.41 (m, 10H, PPh$_2$). ^{13}C NMR (150 MHz in THF-d$_8$): δ = 12.5 (SiCH*Me*$_2$), 17.7 (Si*C*H Me$_2$), 95.7 (Cp-*C*), 98.4 (Cp-*C*), 109.0 (Cp-*C*), 126.4 (PPh$_2$), 127.1 (Ph), 132.9 (Ph), 142.9 (Ph-*ipso*), 144.8 (Cp-*C*PPh$_2$), 145.0 (Cp-*C*OSi). ^{31}P NMR (THF-d$_8$, 242 MHz): δ –17.2.

Iron(II) dichloride (175 mg, 1.38 mmol) was dissolved in THF (20 ml). Lithium [(1-tri-*iso*-propylsilyloxy)-3-diphenylphosphino]cyclopentadienide (1.18 g, 2.75 mmol) was dissolved in THF (20 ml) in a different flask and was cooled to –80 °C. The solution of the lithium salt was transferred to the suspension of FeCl$_2$. The mixture was allowed to warm to room temperature overnight and was stirred under reflux for further 2 hours. The solvent was removed under vacuum and the residue was poured in pentane to afford a brown oil as a 1:1 mixture of *rac* and *meso* **6-r** diastereomers which cannot be separated by the method previously used for **5** (yield 53%, 313 mg, 0.73 mmol). HR-MS (ESI$_{pos}$, DCM/MeOH, m/z): calc. $C_{52}H_{69}FeO_2P_2Si_2^+$ [M+H]$^+$ 899.36023, found 899.36141. Anal. Calcd.: C, 69.47; H, 7.62; Found: C, 68.91; H, 7.89. ^{1}H NMR (CDCl$_3$, 300 MHz): δ 1.06 (m, 36H, CHMe$_2$), 1.08 (m, 6H, CHMe$_2$), 3.28 (m, 1H, Cp-*H*), 3.49 (m, 1H, Cp-*H*), 3.94 (m, 2H, Cp-*H*), 4.06 (m, 1H, Cp-*H*), 4.13 (m, 1H, Cp-*H*), 7.19-7.32 (m, 20H, PPh$_2$). ^{13}C{^{1}H}(CDCl$_3$, 75 MHz): δ 12.2 (s, *C*HMe$_2$), 12.3 (s, *C*HMe$_2$), 17.9 (s, CH*Me*$_2$), 64.8 (pt, J$_{CP}$ = 2.2 Hz, Cp), 64.9 (m, Cp-*C*),67.1 (t, J$_{CP}$ = 15.5 Hz, Cp-*C*), 67.6 (d, J$_{CP}$ = 57.8 Hz, Cp-*C*), 67.9 (m, Cp-*C*), 71.7 (dd, ^{1}J$_{CP}$ =54.8, 9.9 Hz, *C1*-Cp), 124.7 (m, Ph-*ipso*), 125.4 (m, Ph-*ipso*), 127.9 (m, Ph), 128.3 (d, J$_{CP}$ = 7.03 Hz), 133.3 (dd, J$_{CP}$ = 19.6, 6.1 Hz, Ph), 134.0 (dd, J$_{CP}$ = 20.1, 9.2 Hz, Ph), 139.0 (dd, J$_{CP}$ = 28.3, 12.0 Hz, Ph-*ipso*), 140.1 (dd, J$_{CP}$ = 11.4, 7.4 Hz, Ph-*ipso*). ^{31}P{^{1}H}(CDCl$_3$, 121.5 MHz, *rac* + *meso*): –16.58, –17.81.

1,1',2,2'-tetrakis(diphenylphosphino)-4,4'-di(*tert*-butyl) ferrocene (11). This compound is commercially available under the name HiersoPHOS-5 (Strem) and alternatively can be synthesized according to literature report.[45]

Complex 7. To a solution of **4-m** (40 mg, 0.06 mmol) in 1 ml of dichloromethane was added a solution of Au(SMe$_2$)Cl (18 mg, 0.06 mmol) in 2 ml of dichloromethane, and the mixture was stirred for 5 min. The solvent was removed under vacuum to afford an orange solid of **7** (yield >98%). HR-MS (ESI$_{pos}$, DCM/MeOH, m/z): calc. $C_{42}H_{44}AuFeP_2^+$ [M-Cl]$^+$ 863.19394, found 863.18945. Anal. Calcd.: C, 56.11; H, 4.93; Found: C, 55.89; H, 4.95. ^{1}H NMR (CD$_2$Cl$_2$, 500 MHz, 253K): δ 0.81 (s, 9H, *t*-Bu), 1.04 (s, 9H, *t*-Bu), 3.83 (s, 1H, Cp), 4.35 (s, 1H, Cp), 4.58 (s, 1H, Cp), 4.99 (s, 1H, Cp), 5.53 (s, 1H, Cp), 7.14 (t, *J* = 7.0 Hz, 2H, Ph), 7.26 (dd, *J* = 7.0 Hz and 4.5 Hz, 2H, Ph),

7.34-7.40 (m, 2H, Ph), 7.42-7.54 (m, 8H, Ph), 7.60-7.78 (m, 4H, Ph). $^{13}C\{^1H\}$ (CD_2Cl_2, 125.77 MHz): because of solubility troubles at 300 K no other signals than solvent were observed. $^{31}P\{^1H\}$(CD_2Cl_2, 202.44 MHz, 253 K): δ 33.3, 39.4 (ABq, 2P, $^2J_{AB}$ = 316 Hz).

Complex 8. To a solution of **4-m** (40 mg, 0.06 mmol) in 1 ml of dichloromethane was added a solution of [Au(SMe_2)Cl] (36 mg, 0.12 mmol) in 2 ml of dichloromethane, and the mixture was stirred for 5 min. The solvent was removed under vacuum to afford an orange solid of **8**. Yield 99%. HR-MS (ESI_{pos}, DCM/MeOH, m/z): calc. $C_{42}H_{44}Au_2FeP_2Cl_1^+$ $[M\text{-}Cl]^+$ 1095.12938, found 1095.12881. Anal. Calcd.: C, 44.59; H, 3.92; Found: C, 43.25; H, 3.88. ^1H NMR (CD_2Cl_2, 500 MHz): δ 1.15 (s, 18H, *t*-Bu), 4.31 (s, 2H, Cp), 4.66 (s, 2H, Cp), 4.59 (s, 2H, Cp), 7.44-7.70 (m, 20H, Ph). Solubility troubles precluded proper $^{13}C\{^1H\}$ (CD_2Cl_2, 125.77 MHz). $^{31}P\{^1H\}$(CD_2Cl_2, 202.44 MHz): δ 28.5 (s, 2P).

Complex 9. To a solution of **5-r** (41 mg, 0.06 mmol) in 1 ml of dichloromethane was added a solution of [Au(SMe_2)Cl] (36 mg, 0.12 mmol) in 2 ml of dichloromethane, and the mixture was stirred for 5 min. The solvent was removed under vacuum to afford a yellow solid as **9** (99%, 67.7 mg) which can be crystallized from pentane diffusion. Satisfactory HR-Mass was not obtained. Anal. Calcd.: C, 38.78; H, 3.87; Found: C, 36.76; H, 3.70 (trace of sulphur coming from SMe_2were also detected). ^1H NMR (CD_2Cl_2, 300 MHz): δ 1.04 (m, 18H, *t*-Bu), 2.27 (s, 6H, Me), 2.37 (s, 3H, Me), 12.40 (S, 3H, Me), 4.40 (s, 2H, Cp), 4.47 (s, 2H, Cp), 4.73 (s, 2H, Cp), 5.97 (m, 2H, furyl), 6.21 (m, 4H, furyl), 6.44 (s, 2H, furyl). Solubility troubles precluded proper $^{13}C\{^1H\}$. $^{31}P\{^1H\}$(CD_2Cl_2, 202.44 MHz): δ –16.9 (s, 2P).

Complex 10. To a solution of (*rac* + *meso*) **6** (54 mg, 0.06 mmol) in 1 ml of dichloromethane was added a solution of [Au(SMe_2)Cl] (36 mg, 0.12 mmol) in 2 ml of dichloromethane, and the mixture was stirred for 5 min. The solvent was removed under vacuum and a mixture of pentane/dichloromethane 1:1 was used to recrystallized an orange solid identified as (*rac*) **10** (yield 40%, 34.8 mg) by single X-ray diffraction and ^{31}P NMR. HR-MS (ESI_{pos}, DCM/MeOH, m/z): calc. $C_{52}H_{68}Au_2ClFeO_2P_2Si^+$ $[M\text{-}Cl]^+$ 1327.25984, found 1327.26218. Anal. Calcd.: C, 45.79; H, 5.03; Found: C, 45.86; H, 5.24 (traces of sulphur coming from SMe_2 were also detected). ^1H NMR ($CDCl_3$, 500 MHz): δ 0.96-0.98 (m, 36H, *i*-Pr), 1.19 (s, 6H, *i*-Pr), 3.52-3.54 (m, 2H, Cp), 4.09-4.11 (m, 2H, Cp), 4.62-4.64 (m, 2H, Cp), 7.19-7.45 (m, 20H, Ph). $^{13}C\{^1H\}$ ($CDCl_3$, 125.77 MHz): δ 11.1, 16.8, 16.9, 64.7, 65.6, 66.2, 66.3, 67.2, 67.4, 67.6, 126.4, 126.5, 127.8, 127.9, 128.1, 128.2, 129.5, 130.2, 130.6, 131.0, 132.2, 132.5, 132.6. $^{31}P\{^1H\}$(CD_2Cl_2, 202.44 MHz): δ 28.9 (s, 2P).

Complex 12. The reaction of **11** (31 mg, 0.03 mmol) with 1 equiv of [Au(SMe_2)Cl] (9 mg, 0.03 mmol) afforded **12** in 99 % yield (37.1 mg) immediately upon mixture in CH_2Cl_2 (or CH_3Cl). Anal. Calcd.: C, 62.55; H, 4.93; Found: C, 61.87; H, 5.65. NMR ^1H (500 MHz, 298 K): δ 0.69 (s, 18H), 4.10 (s, 2H), 4.18 (s, 2H), 6.7-7.2 (m, 40H). NMR $^{13}C\{1H\}$ (125.77 MHz, 298 K): δ 31.2, 70.5, 71.5, 76.2, 77.6, 78.1, 125.4, 127.9, 127.9, 128.0, 128.0, 128.2, 128.2, 128.3, 128.3, 128.7, 128.8, 128.9, 128.9, 129.1, 129.4, 129.5, 129.5, 129.8, 130.1, 130.5, 130.7, 131.7, 132.5, 132.9, 134.4, 135.0, 135.3, 135.5, 136.2, 136.6, 136.8, 136.8, 138.2. NMR $^{31}P\{^1H\}$ (202.44 MHz, 298 K): δ–18.5 (m), 10.4 (m).

Complex 13. The complexation of **11** (31 mg, 0.03 mmol) and 3 equiv of [Au(SMe_2)Cl] (27 mg, 0.09 mmol) afforded complex which was isolated in 33% yield (50.9 mg) after purification. NMR ^1H ($CDCl_3$, 500 MHz, 298 K):

δ 0.87 (s, 18H), 4.46 (s, 2H), 4.83 (s, 2H), 6.6-7.7 (m, 36H), 8.67 (m, 4H). NMR $^{13}C\{^{1}H\}$ (125.77 MHz, 298 K): δ 30.6, 72.1, 77.9, 128.9, 129.4, 130.1, 131.8, 132.1, 133.2, 133.3, 135.1, 136.9. NMR $^{31}P\{^{1}H\}$ (202.44 MHz, 298 K): δ 19.1 (m, AA'BB').

Complex 14. The complexation of **11** (31 mg, 0.03 mmol) and 2 equiv of [Au(SMe_2)Cl] (18 mg, 0.06 mmol) affords **14** in 33 % yield from ^{31}P, in an intractable mixture with **12** and **13** (1/1/1).

X-ray Diffraction Analysis. Intensity data for all the complexes were collected on a Bruker APEX II CCD diffractometer at 115 K with Mo K_a radiation. Using Olex2 program[46] the structures were solved with the shelXT[47] and refined with the shelXL[48] refinement package using least-squares minimization on F^2. All non-hydrogen atoms were refined with anisotropic thermal parameters. Hydrogen atoms were included in their calculated positions and refined with a riding model. Special refinement details for some complexes are given now. The complex **8** crystallizes with 1.5 dichloromethane solvent molecules. These molecules were included as rigid groups in the model. One was disordered around an inversion center and refined with an occupation factor of 0.5 while the other was also found disordered over two positions and refined with converged multiplicities of 0.72/0.28. The complex **9** crystallizes with one dichloromethane molecule that is also disordered around an inversion center and refined with an occupation factor of 0.5 (the complex being located on a *C2* axis, the ratio complex/solvent is 1/1). The gold atom in complex **12** is found disordered over two positions (occupancies 0.90/0.10) the minor component was refined with a RIGU restraint. Two dichloromethane are present in the asymmetric unit, they were included as rigid groups with the Uij components restrained by ISOR, and one of the carbon atom left isotropic. The compound **14** presents also some disorders: a third Au-Cl group is linked to a phosphorus atom, this group was anisotropically refined with a converged occupancy of 0.11. Three dichloromethane molecules are present in the asymmetric unit; all of them are disordered over two positions and their occupancies factors converged to 0.73/0.42, 0.58/0.42 and 0.89/0.11.

ASSOCIATED CONTENT

Supporting Information

Ferrocenylphosphines and gold complexes characterization data. This material is available free of charge via the Internet at http://pubs.acs.org."

AUTHOR INFORMATION

Corresponding Author

jean-cyrille.hierso@u-bourgogne.fr

Author Contributions

The manuscript was written through contributions of all authors. All authors have given approval to the final version of the manuscript.

Notes

The authors declare no competing financial interest

ACKNOWLEDGMENT

The authors acknowledge support provided by the Université de Bourgogne (MESRT PhD Grant for VR), Région Bourgogne (PARI I-SMT8 and PARI II-CDEA), CNRS (3MIM) and the Institut Universitaire de France (IUF). A. Job and S. Royer (ICMUB, Dijon) are thanked for the syntheses of phosphine ligands. Calculations were performed using HPC resources from DSI-CCUB (Université de Bourgogne).

REFERENCES

(1) (a) Schmidbaur, H.; Schier, A. *Chem. Soc. Rev.* **2008**, *37*, 1931. (b) Schmidbaur, H.; Schier, A. *Chem. Soc. Rev.* **2012**, *41*, 370. (c) Sculfort, S.; Braunstein, P. *Chem. Soc. Rev.* **2011**, *40*, 2741.

(2) Gómez-Suárez, A.; Nolan, S. P. *Angew. Chem. Int. Ed.* **2012**, *51*, 8156.

(3) Naked Au_2 has a calculated bond length Au–Au of 2.546 Å, see: Weinberger, D. S.; Melaimi, M.; Moore, C. E.; Rheingold, A. L.; Frenking, G.; Jerabek, P.; Bertrand, G. *Angew. Chem. Int. Ed.* **2013**, *52*, 8964.

(4) (a) Modern Gold Catalyzed Synthesis; Hashmi, A. S. K., Toste, D. F., Ed.; Wiley-VCH: Weinheim, Germany, 2012. (b) Gold: Progress in Chemistry, Biochemistry and Technology; Schmidbaur, H., Ed.; John Wiley & Sons: Chichester, U.K., 1999. (c) Pyykkö, P. *Angew. Chem. Int. Ed.* **2004**, *43*, 4412. (d) Yam, V. W. W.; Cheng, E. C. C. *Chem. Soc. Rev.* **2008**, *37*, 1806.

(5) Schmidbaur, H.; Müller, G. G. *Angew. Chem. Int. Engl.* **1988**, *27*, 417.

(6) Moriya, M.; Fröhlich, R.; Kehr, G.; Erker, G.; Grimme, S. *Chem. Asian. J.* **2008**, *3*, 753.

(7) Hill, D. T.; Girard, G. R.; McCabe, F. L.; Johnson, R. K.; Stupik, P. D.; Zhang, J. H.; Reiff, W. M.; Eggleston, D. S. *Inorg. Chem.* **1989**, *28*, 3529.

(8) Smyth, D. R.; Hester, J.; Young, V. G. Jr; Tiekink, E. R. T. *CrystEngComm.* **2002**, *4*, 517.

(9) Crespo, O.; Gimeno, M. C.; Laguna, A.; Kulcsar, M.; Silvestru, C. *Inorg. Chem.* **2009**, *48*, 4134.

(10) Ho, S. Y.; Tiekink, E. R. *Acta Cryst. E* **2009**, *65*, m1466.

(11) Ho, S. Y.; Cheng, E. C.-C.; Tiekink, E. R. T.; Yam, V. W.-W. *Inorg. Chem.* **2006**, *45*, 8165.

(12) Xu, H.-B.; Zhang, L.-Y.; Ni, J.; Chao, H.-Y.; Chen, Z.-N. *Inorg. Chem.* **2008**, *47*, 10744.

(13) Punji, B.; Mague, J. T.; Balakrishna, M. S.; *Inorg. Chem.* **2007**, *46*, 10268-10275.

(14) (a) Hierso, J.-C.; Fihri, A.; Ivanov, V. V.; Hanquet, B.; Pirio, N.; Donnadieu, B.; Rebière, B.; Amardeil, R.; Meunier, P. *J. Am. Chem. Soc.* **2004**, *126*, 11077. (b) Hierso, J.-C.; Evrard, D.; Lucas, D.; Richard, P.; Cattey, H.; Hanquet, B.; Meunier, P. *J. Organomet. Chem.* **2008**, *693*, 574. (c) Mom, S.; Beaupérin, M.; Roy, D.; Royer, S.; Amardeil, R.; Cattey, H.; Doucet, H.; Hierso, J.-C. *Inorg. Chem.* **2011**, *50*, 11592.

(15) For Pd-catalyzed coupling reactions, see: (a) Roy, D.; Mom, S.; Royer, S.; Lucas, D.; Hierso, J.-C.; Doucet, H. *ACS Catal.* **2012**, *2*, 1033. (b) Zinovyeva, V. A.; Mom, S.; Fournier, S.; Devillers, C. H.; Cattey, H.; Doucet, H.; Hierso, J.-C.; Lucas, D. *Inorg. Chem.* **2013**, *52*, 11923. (c) Mom, S.; Platon, M.; Cattey, H.; Spencer, H. J.; Low, P. J.; Hierso, J.-C. *Catal. Commun.* **2014**, *51*, 10. (d) Platon, M.; Roger, J.; Royer, S.; Hierso, J.-C. *Catal. Sci. Technol.* **2014**, *4*, 2072.

(16) (a) Beaupérin, M.; Fayad, E.; Amardeil, R.; Cattey, H.; Brandès, S.; Meunier, P.; Hierso, J.-C. *Organometallics* **2008**, *27*, 1506. (b) Beaupérin, M.; Job, A.; Cattey, H.; Royer, S.; Meunier, P.; Hierso, J.-C. *Organometallics* **2010**, *29*, 2815.

(17) (a) Gimeno, M. C.; Laguna, A.; Sarroca, C. *Inorg. Chem.* **1993**, *32*, 5926-5932. (b) Canales, F.; Gimeno, M. C.; Jones, P. G.; Laguna, A.; Sarroca, C. *Inorg. Chem.* **1997**, *36*, 5206.

(18) (a) Houlton, A.; Mingos, D. M. P.; Murphy, D. M.; Williams, D. J.; Phang, L.-T.; Hor, T. S. A. *J. Chem. Soc. Dalton Trans.* **1993**, 3629; (b) Phang, L.-T.; Hor, T. S. A.; Zhou, Z.-Y.; Mak, T. C. W. *J. Organomet. Chem.* **1994**, *469*, 253.

(19) (a) Houlton, A.; Roberts, R. M. G.; Silver, J.; Parish, R. V. *J. Organomet. Chem.* **1991**, *418*, 269. (b) Viotte, M. Gautheron, B; Kubicki, M. M.; Mugnier, Y.; Parish, R. V. *Inorg. Chem.* **1995**, *34*, 3465.

(20) Gimeno, M. C.; Laguna, A. *Chem. Rev.* **1997**, *97*, 511.

(21) Devillard, M.; Nicolas, E.; Appelt, C.; Backs, J.; Mallet-Ladeira, S.; Bouhadir, G.; Slootweg, J. C.; Uhl, W.; Bourissou, D. *Chem. Commun.* **2014**, *50*, 14805.

(22) Commercially available from Strem Chemicals under the trade name HiersoPHOS-5.

(23) Hierso, J.-C. *Chem. Rev.* **2014**, *114*, 4838.

(24) Malkina, O. L.; Malkin V. G. *Angew. Chem. Int. Ed.* **2003**, *42*, 4335.

(25) Contreras, R. H.; Gotelli, G.; Ducati, L. C.; Barbosa, T. M.; Tormena, C. F. *J. Phys. Chem. A* **2010**, *114*, 1044.

(26) Soncini, A.; Lazzeretti, P. *J. Chem. Phys.* **2003**, *119*, 1343.

(27) Beaupérin, M.; Smaliy, R.; Cattey, H.; Meunier, P.; Ou, J.; Toy, P. H.; Hierso, J.-C. *Chem. Commun.* **2014**, *50*, 9505.

(28) Beaupérin, M.; Smaliy, R.; Cattey, H.; Meunier, P.; Ou, J.; Toy, P. H.; Hierso, J.-C. *ChemPlusChem,* **2015**, *80*, 119.

(29) Stoccoro, S.; Alesso, G.; Cinellu, M. A.; Minghetti, G.; Zucca, A.; Manassero, M.; Manassero, C. *Dalton Trans*. **2009**, 3467.

(30) Feng, G.; Conley, M. P.; Jordan, R. F. *Organometallics* **2014**, *33*, 4486.

(31) Cowie, B. E.; Tsao, F. A.; Emslie, D. J. H. *Angew. Chem. Int. Engl.* **2015**, *54*, 2165.

(32) Zank, J.; Schier, A.; Schimdbaur, H. *J. Chem. Soc. Dalton Trans* **1999**, 415.

(33) (a) Jones, P. G.; Sheldrick, G. M.; Muir, M. M.; Pulgar, L. B. *J. Chem. Soc. Dalton* **1982**, 2123. (b) Attar, S.; Bearden, W. H.; Alcock, N. W.; Nelson, J. H. *Inorg. Chem.* **1990**, 29, 425. (c) Baker, R. T.; Calabrese, J. C.; Westcott, S. A. *J. Organomet. Chem.* **1995**, *498*, 109. (d) Caruso, F.; Rossi, M.; Tanski, J.; Pettinari, C.; Marchetti, F. *J. Med. Chem.* **2003**, *46*, 1737. (e) Lubbe, G. ; Frolich, R.; Kehr, G.; Erker, G. *Inorg. Chim. Acta* **2011**, *369*, 223. (f) Jenkins, D. E.; Sykora, R. E.; Assefa, Z.; *Inorg. Chim. Acta* **2013**, *406*, 293. (g) Bardaji, M.; de la Cruz, M. T.; Jones, P.G.; Laguna, A.; Martinez, J.; Villacampa, M. D. *Inorg. Chim. Acta* **2005**, *358*, 1365. (h) Houlton, A.; Mingos, D. M. P.; Murphy, D. M.; Williams, D. J. *Acta Crystallogr., Sect. C*. **1995**, 51. (i) Dieleman, C. B.; Matt, D.; Harriman, A. *Eur. J. Inorg. Chem*. **2000**, 831-834. (j) Dempsey, J. L.; Esswein, A. J.; Manke, D. R.; Rosenthal, J.; Soper, J. D.; Nocera, D. G. *Inorg. Chem*. **2005** ,*44*, 6879-6892.

(34) The transfer of one Au(I) chloride unit between two molecules of dinuclear compound **14** may give rise to a mixture of mononuclear **12** and trinuclear **13** compounds. The establishment of stable 1:1:1 equilibrium between **12-14** was repeatedly observed but its origin is still unclear.

(35) (a) Gramage-Doria, R.; Armspach, D.; Matt, D. *Angew. Chem. Int. Ed.* **2011**, *50*, 1554. (b) Gramage-Doria, R.; Armspach, D.; Matt, D; Toupet, L. *Dalton Trans.* **2012**, *41*, 8786.

(36) (a) Becke, A. D.; Edgecombe, K. E. *J. Chem. Phys.* **1990**, *92*, 5397; (b) Silvi, B.; Savin, A. *Nature* **1994**, *371*, 683; (c) Noury, S.; Krokidis, X.; Fuster, F.; Silvi, B. *Comput. Chem.* **1999**, *23*, 597.

(37) Gillespie, R. J.; Nyholm, R. S. *Q. Rev. Chem. Soc.* **1957**, *11*, 339.

(38) Frisch, M. J. *et al.*, *Gaussian 09, Revision D.01*, Gaussian, Inc., Wallingford CT, **2009**.

(39) (a) Lee, C.; Yang, W.; Parr, R. G. *Phys. Rev. B* **1988**, *37*, 785. (b) Becke, A. D. *J. Chem. Phys.* **1993**, *98*, 5648.

(40) Canal Neto, A.; Jorge F. E. *Chem. Phys. Lett.* **2013**, *582*, 158.

(41) Rappoport, D.; Furche, F. *J. Chem. Phys.* **2010**, *133*, 134105.

(42) (a) Hehre, W. J.; Ditchfield, R.; Pople J. A. *J. Chem. Phys.* **1972**, 56, 2257. (b) Clark, T.; Chandrasekhar, J.; Spitznagel, G. W.; Schleyer, P. v. R. *J. Comp. Chem.* **1983**, *4*, 294. (c) Francl, M. M.; Petro, W. J.; Hehre, W. J.; Binkley, J. S.; Gordon, M. S.; DeFrees, D. J.; Pople, J.A. *J. Chem. Phys.* **1982**, *77*, 3654. (d) Frisch, M. J.; Pople, J. A.; Binkley J. S. *J. Chem. Phys.* **1984**, *80*, 3265.

(43) Humphrey, W., Dalke, A. Schulten, K. *J. Mol. Graph.* **1996**, *14*, 33.

(44) Broussier, R.; Bentabet, E.; Mellet, P.; Blacque, O.; Boyer, P.; Kubicki, M. M.; Gautheron, B. *J. Organomet Chem.* **2000**, *598*, 365.

(45) Broussier, R.; Bentabet, E.; Amardeil, R.; Richard, P.; Meunier, P.; Kalck, P.; Gautheron, B. *J. Organomet Chem.* **2001**, *637-639*, 126.

(46) Dolomanov O. V.; Bourhis, L. J.; Gildea, R. J.; Howard, J. A. K.; Puschmann H. *J. Appl. Cryst.,* **2009**, *42*, 339.

(47) Sheldrick, G. M., *Acta Cryst.*, **2015**, *A71*, 3.

(48) (a) Sheldrick G. M., *Acta Cryst*., **2008**, *A64*, 112; (b) Sheldrick, G. M., *Acta Cryst.*, **2015**, *C27*, 3.

FOR TABLE OF CONTENTS ONLY

Table of Contents Synopsis

Steric conformation control of ferrocene backbone in bis- and tetrakis(phosphino) ferrocenes favors intramolecular aurophilic interactions between $Au^{I}Cl$ fragments in polynuclear gold complexes. Introduction of *tert*-butyl groups on the ferrocene rings facilitates Au···Au aurophilic bonds in diphosphine complexes. In tetraphosphine complexes, dynamic shuttling of aurophilic dinuclear edifices between phosphino groups was evidenced, as well as a rare $^{31}P–^{31}P'$ nonbonded TS nuclear spin coupling transferred via phosphorus lone-pair and Au–P' σ bond.

Table of Contents Graphic: 8.5 cm by 4.75 cm